

INTERIOR NOISE ANALYSIS OF A ROTARY WING AIRCRAFT BY HYBRID
STATISTICAL ENERGY AND FINITE ELEMENT ANALYSIS

A THESIS SUBMITTED TO
THE GRADUATE SCHOOL OF NATURAL AND APPLIED SCIENCES
OF
MIDDLE EAST TECHNICAL UNIVERSITY

BY

RECEP HİLMİ KANLIOĞLU

IN PARTIAL FULFILLMENT OF THE REQUIREMENTS
FOR
THE DEGREE OF MASTER OF SCIENCE
IN
MECHANICAL ENGINEERING

SEPTEMBER 2018

Approval of the thesis:

**INTERIOR NOISE ANALYSIS OF A ROTARY WING AIRCRAFT BY
HYBRID STATISTICAL ENERGY AND FINITE ELEMENT ANALYSIS**

submitted by **RECEP HİLMİ KANLIOĞLU** in partial fulfillment of the requirements for the degree of **Master of Science in Mechanical Engineering Department, Middle East Technical University** by,

Prof. Dr. Halil Kalıpçılar
Dean, Graduate School of **Natural and Applied Sciences**

Prof. Dr. M.A.Sahir Arıkan
Head of Department, **Mechanical Engineering**

Prof. Dr. Mehmet Çalışkan
Supervisor, **Mechanical Engineering Dept., METU**

Examining Committee Members:

Assoc. Prof. Dr. Yiğit Yazıcıoğlu
Mechanical Engineering Dept., METU

Prof. Dr. Mehmet Çalışkan
Mechanical Engineering Dept., METU

Assist. Prof. Dr. M. Bülent Özer
Mechanical Engineering Dept., METU

Assist. Prof. Dr. Orkun Özşahin
Mechanical Engineering Dept., METU

Assist. Prof. Dr. Zühre Sü Gül
Architecture Dept. , Bilkent University

Date: 03.09.2018

I hereby declare that all information in this document has been obtained and presented in accordance with academic rules and ethical conduct. I also declare that, as required by these rules and conduct, I have fully cited and referenced all material and results that are not original to this work.

Name, Last name: Recep Hilmi KANLIOĞLU

Signature : _____

ABSTRACT

INTERIOR NOISE ANALYSIS OF A ROTARY WING AIRCRAFT BY HYBRID STATISTICAL ENERGY AND FINITE ELEMENT ANALYSIS

Kanlıoğlu, Recep Hilmi

MSc., Department of Mechanical Engineering

Supervisor: Prof. Dr. Mehmet Çalışkan

September 2018, 95 pages

Prediction of interior noise level within a helicopter fuselage is an important design aspect considering competition in the aviation global market combined with customer's comfort expectations. Especially, in the development phase of a new product, accurate vibro-acoustic models are required to give an engineering assessment to guide the design. The objective of this study is to review noise-generating mechanism on helicopters and vibro-acoustic analysis techniques, and to build two different predictive Statistical Energy Analysis (SEA) models for a conventional type of helicopter. One approach involves SEA where structures are modelled by SEA subsystems, while the other approach is hybrid FEM-SEA where stiffer components having few modes at the low-to-mid frequency range are constructed with finite element while the rest represented by SEA subsystems. Excitations due to the main gearbox is taken from flight measurements on similar helicopters. Turbulent Boundary Layer (TBL), engine airborne noise and main and tail rotor excitations are also applied as main sources of interior noise. Through the analysis, sound

pressure levels for the cruise condition are evaluated in the frequency range of interest up to 16000 Hz by commercial software.

Keywords: Statistical Energy Analysis, Helicopter, Interior Noise.

ÖZ

DÖNER KANATLI BİR HAVA ARACININ İÇ GÜRÜLTÜSÜNÜN MELEZ İSTATİSTİKSEL ENERJİ VE SONLU ELEMANLAR YÖNTEMİ İLE ANALİZİ

Kanlıođlu, Recep Hilmi

Yüksek Lisans, Makina Mühendisliđi Bölümü

Tez Yöneticisi: Prof. Dr. Mehmet Çalıřkan

Eylül 2018, 95 sayfa

Küresel havacılık pazarındaki rekabet ve müşterilerin konfor beklentileri nedeniyle helikopter iç kabin gürültü düzeyi öngörüsü bir tasarım kriteri olarak önemlidir. Özellikle yeni ürün geliştirme safhasında, doğru vibroakustik modelleri mühendislik değerlendirmesi ile tasarıma yön vermesi açısından gerekir. Bu çalışmanın amacı helikopterdeki gürültü üretici mekanizmaları ve vibroakustik analiz tekniklerini gözden geçirmek ve konvansiyonel bir helikopter tipi için iki farklı istatistiksel enerji analizi (İEA) modeli oluşturmaktır. Bir yaklaşımda İEA altsistemleri ile modellenirken, diğerinde az sayıda titreşim biçimine sahip katı yapıların sonlu elemanlar, geriye kalan yapıların ise İEA altsistemleri ile modellendiđi hibrit modeldir. Ana dişli kutusundan gelen tahrikler benzer helikopterlerden ölçülen değerler alınarak hesaba katılmıştır. Türbulanslı sınır katmanı, havadan taşınan motor gürültüsü; ana ve kuyruk pervane uyarıları ayrıca ana gürültü kaynakları olarak modele eklenmiştir. Analiz boyunca düz seyir koşulu için ses

basınç seviyeleri, 16000 Hz'e kadar olan frekans aralığında, ticari bir analiz yazılımı ile hesaplanmıştır.

Anahtar Sözcükler: İstatiksel Enerji Analizi, Helikopter, Kabin içi Gürültüsü.

To My Family

ACKNOWLEDGMENTS

The author wishes to express his deepest gratitude to his supervisor Prof. Dr. Mehmet Çalışkan for his guidance, advice, criticism, encouragements and insight throughout the research.

I would like to gratefully acknowledge Evren Eyüp Taşkınoğlu and Fatih Özbakış from Turkish Aerospace Industry (TAI) for invaluable support.

The author also like to thank his family for their invaluable support and unceasing patience because of my nervous behavior during the thesis study.

TABLE OF CONTENTS

ABSTRACT	v
ÖZ	vii
ACKNOWLEDGMENTS.....	x
TABLE OF CONTENTS.....	xi
LIST OF TABLES	xiii
LIST OF FIGURES	xiv
LIST OF SYMBOLS AND ABBREVIATIONS	xvii
CHAPTERS	1
1.INTRODUCTION.....	1
1.1. Noise Generating Mechanism on Helicopters.....	1
1.2. Methods for Helicopter Interior Noise Prediction.....	7
1.3. Choice of Approach.....	12
1.4. Motivations and Objectives.....	12
2.STATISTICAL ENERGY ANALYSIS	13
2.1. A Brief Introduction and Literature Survey	13
2.2. Basis and Methodology of SEA	18
2.3 Basis and Methodology of FEM-SEA Hybrid Method.....	30
3.APPLICATION OF SEA METHOD.....	35
3.1 Aircraft Based Applications of SEA	35
3.2 General Overview of Simulated Rotorcraft	39
3.3 Modeling Process	41
3.3.1 SEA Model.....	41
3.3.1.1 Dynamic Properties and Loss Factors of SEA Subsystems	57
3.3.2 Hybrid Model.....	60
4.ANALYSIS AND RESULTS.....	65

4.1	Power Inputs.....	65
4.1.1	Main and Tail Rotor Noise.....	67
4.1.2	TBL Noise.....	68
4.1.3	Main Gear Box Noise.....	70
4.1.4	Engine Noise.....	73
4.2	Prediction of Helicopter Cabin Noise Level.....	74
4.2.1	SEA Model Results.....	74
4.2.2	FEM-SEA Hybrid Model Results.....	77
5.	CONCLUSIONS AND FUTURE WORK.....	85
5.1.	Discussion of Results.....	85
5.2.	Summary and Conclusions.....	87
5.3.	Recommendations for Future Work.....	89
6.	REFERENCES.....	91

LIST OF TABLES

TABLES

Table 1.1 Comparison of simulation techniques	11
Table 3.1 Cabin dimensions	40
Table 3.2 Main characteristics of TLUH	40
Table 3.3 Wave fields of SEA subsystems.....	45
Table 3.4 Required ribbed plate description.....	47
Table 3.5 Front fuselage SEA subsystems identification.....	48
Table 3.6 Beam properties of “front lower panel”.....	49
Table 3.7 Mid fuselage SEA systems identification.....	50
Table 3.8 Beam properties of “mid fuselage lower panel1-2”.....	51
Table 3.9 Absorption coefficient for Flexed Foam.....	52
Table 3.10 Rear fuselage SEA systems identification.....	53
Table 3.11 Beam properties of “rear fuselage upper panel”.....	54
Table 3.12 Tail fuselage SEA systems identification.....	55
Table 3.13 Beam properties of “tail fuselage upper panel”.....	55
Table 4.1 Flight condition.....	66
Table 4.2 Power spectral density formulae for different conditions.....	69
Table 5.1 MIL-STD-1474D Sound Pressure Limits.....	88

LIST OF FIGURES

FIGURES

Figure 1.1 Main noise sources of helicopter.....	3
Figure 1.2 Structure-borne noise travelling mechanism.....	3
Figure 1.3 Airborne noise travelling mechanism.....	4
Figure 1.4 Airborne and structure-borne paths of helicopter noise.....	4
Figure 1.5 Noise travelling paths inside helicopter cabin (Caillet, Marrot, Malburet, Carmona, 2005).....	5
Figure 1.6 Noise characteristic of helicopter cabin (Mucchi, Pierro, Vecchio, 2005).....	6
Figure 1.7 Noise classification of helicopter cabin (Mucchi, Vecchio, 2009).....	6
Figure 1.8 Relation between frequency and DOF in fluid and structural domain (Davidsson, 2004).....	9
Figure 2.1 Linear resonators coupled by spring, mass, and gyroscopic elements (Lyon, 1995).....	14
Figure 2.2 Simple illustration of coupled plates.....	18
Figure 2.3 Wave approach to coupling of 1D elements (Lyon, 1995).....	26
Figure 2.4 Wave analysis of a line junction (Lyon, 1995).....	27
Figure 2.5 Schematic representation of hybrid system (Shorter, Langley, 2005).....	31
Figure 3.1 General view of Turkish Light Utility Helicopter.....	39
Figure 3.2 Imported finite element model of TLUH.....	42
Figure 3.3 Complete SEA model of TLUH.....	43
Figure 3.4 SEA Model with exterior acoustic space.....	43

Figure 3.5 SEA model with junctions.....	46
Figure 3.6 Front fuselage SEA subsystems.....	48
Figure 3.7 Mid fuselage SEA subsystems.....	50
Figure 3.8 Acoustically treated components.....	52
Figure 3.9 Rear fuselage SEA subsystems.....	53
Figure 3.10 Tail fuselage SEA subsystems.....	54
Figure 3.11 Internal SEA cavities.....	56
Figure 3.12 External SEA cavities.....	56
Figure 3.13 Mode count for front fuselage SEA subsystems.....	58
Figure 3.14 Mode count for mid fuselage SEA subsystems.....	59
Figure 3.15 Overall view of the hybrid FE-SEA model of the helicopter.....	60
Figure 3.16 Junctions of hybrid FE-SEA Model.....	61
Figure 3.17 Mode count for front fuselage FE subsystems.....	62
Figure 3.18 Mode count for mid fuselage FE subsystems.....	62
Figure 4.1 External excitations.....	66
Figure 4.2 Near field pressure levels of main and tail rotors.....	68
Figure 4.3 UH-1D measured sound pressure levels.....	71
Figure 4.4 CH-47A measured sound pressure levels.....	72
Figure 4.5 MGB airborne noise estimation of TLUH.....	73
Figure 4.6 Engine exhaust measured pressure levels.....	74
Figure 4.7 SEA estimation of TLUH passenger cabin without NCT.....	75
Figure 4.8 Comparison of helicopter cabin noise levels with similar helicopters of comparable power.....	76

Figure 4.9 Comparison of SEA sound pressure levels with and without NCT.....76

Figure 4.10 Hybrid estimation of TLUH passenger cabin without NCT.....77

Figure 4.11 Hybrid-SEA comparison.....78

Figure 4.12 Sound Pressure Level- Mode Count comparison.....79

Figure 4.13 Energy distribution in SEA subsystem at 250 Hz.....80

Figure 4.14 Energy distribution in hybrid FE-SEA model at 250 Hz81

Figure 4.15 Energy level of SEA subsystems82

Figure 4.16 Energy level of FE- SEA subsystems82

Figure 5.1 Sound energy flow in outside cavities at 1000 Hz.....86

Figure 5.2 Comparison of SEA cabin noise results with MIL standard.....89

LIST OF SYMBOLS AND ABBREVIATIONS

A	Area
B	Matrix B
c_0	Speed of Sound In Air
c_B	Bending Wave Speed
c_φ	Phase Speed
c_g	Energy Group Speed
C	Peak Response Amplitude
DR	Decay Rate
D_d	Dynamic Stiffness Matrix
δ_{BC}	Boundary Condition Constant
Δ_f	Half Power Bandwidth
$\Delta\omega$	Band Width
E	Elastic (Young's) Modulus
E_i	Subsystem Energy
η_i	Damping Loss Factor
η_{ij}	Coupling Loss Factor
f	Center Frequency of the Band in Hz
f_c	Critical Frequency
f_{rev}	Reverberant Field Force
F	Force
G	Conductance
h	Thickness

hp	Horse Power
J	Torsional Moment of Rigidity
I_{ii}	Polar Area Moment of Inertia
Q_{zz}	Torsion Constant
k_N	Wave Number per unit length
K_0	Bulk Modulus of the Fluid
KEAS	Speed (mile per hour)
L	Length
L_E	Energy Level
L_p	Sound Pressure Level
L_w	Sound Pressure Level
m	Mass
M	Number of Subsystems
μ	Poisson's Ratio
N	Number of Modes
Δ_N	Number of Modes in frequency band Δ_ω
n	Modal Density
$n(\omega)$	Modal Density (rad/s)
$n(f)$	Modal Density (Hz)
ω	Center Frequency of the Band in rad/s
P	Pressure
Π_{in}	Power Input to Subsystem i
Π_{diss}	Power Dissipated Within Subsystem i
Π_{ij}	Power Flow From Subsystem I to Subsystem j
$\langle p^2 \rangle$	Mean Square Acoustic Pressure

r	Amplitude of Reflection coefficient
rpm	Revolution per Minute
R	System Impedance
Re	Reynolds Number
S	Surface Area of an Acoustic Volume
ρ	Density
t	Time
T_R	Reverberation Time
T_{12}	Decay Rate Time
τ_{ij}	Transmission Coefficient
α	Radius
U	Volume Velocity
U_0	Free stream flow velocity
V	Volume
$\langle v^2 \rangle$	Mean square Velocity
$\nu \nu$	Fluid kinematic viscosity at flight altitude
X_0	Distance from the leading edge of the TBL to the center of pressure load on the surface of the subsystem
SEA	Statistical Energy Analysis
FEM	Finite Element Model
BEM	Boundary Element Method
CLF	Coupling Loss Factor
TBL	Turbulent Boundary Layer
NCT	Noise Control Treatment
NRS	Noise Reduction Constant
MGB	Main Gear Box
TLUH	Turkish Light Utility Helicopter

CAE	Computer Aided Engineering
ECS	Environmental Control System
MIL	Military Standard

CHAPTER 1

INTRODUCTION

Sound is generated from vibrational behavior of air. It is kind of mechanical energy that stirs up the pressure in the air. The larger amplitude of sound wave makes the sound louder and could be harsh to the human ears. Excessive and undesirable sound is called as noise. There are regulations that set limits to maximum noise levels caused long-lasting hearing loss [1].

Noise and vibration issues have been evolving as a quality indicator in time. Especially for air platforms, both noise pollution legislations and customer desire cause to reduce aircraft exterior and interior noise levels and also vibration. Among aircraft counterparts, helicopter is the noisiest craft. Nowadays, they are used in various segments, such as rescue operations, military missions, transfer functions or private use. Therefore, the competition in the global market combined with comfort expectations require an acoustical study in detail. The noise sources, analysis methods should be well known to propose effective solution for reducing high noise levels.

1.1. Noise Generating Mechanism on Helicopters

Rotating sources are of interest in laboratory for many years. When propeller powered aircraft brings into use, sound radiation from rotating sources have attracted attention of

researchers. With huge rotor systems, helicopters are excessive sources of noise and it becomes a substantial problem that makes deterrent air travel for many persons [2]. There is a complete pandemonium of sounds in the cabin of the rotorcraft. It makes sometimes conversation fully impossible. Consequently, noise diagnostics and treatments should be applied to refine acoustical performance. There has been an appreciable decrease in noise levels over the years by improving the noise reduction technologies. The improvements of helicopter interior noise can cover the following features [3];

- Determination of noise sources and solutions
- Attaining driver's expectation of acoustic comfort
- Reaching passengers' ride acoustic comfort targets
- Legislation approval
- Health safety approval

Excessive structural vibrations, physical mechanisms and systems as well as insufficient sound reduction treatments on interior cabin walls could be the reasons of interior noise. It is important to identify the root of the noise that cause uncomfortable perception. For that reason, in the early phase of design development, the sources, transfer paths and receivers have to be identified and analyzed. Relief improvements upon troubleshooting may be developed after the analysis.

Helicopter has complex noise sources as illustrated in Figure 1.1. Transmission drive system, main and tail rotors, engines and aerodynamic pressure excitation are the main primary sources of cabin noise extending over low to high bands in the frequency range. The sound generation from fans, pumps and environmental control system (ECS) mostly are suppressed/disappear under dominant primary sources. Therefore they can be overlooked. The location with respect to passenger cabin and strength of noise sources also affects both noise levels and noise quality in the interior cabin.

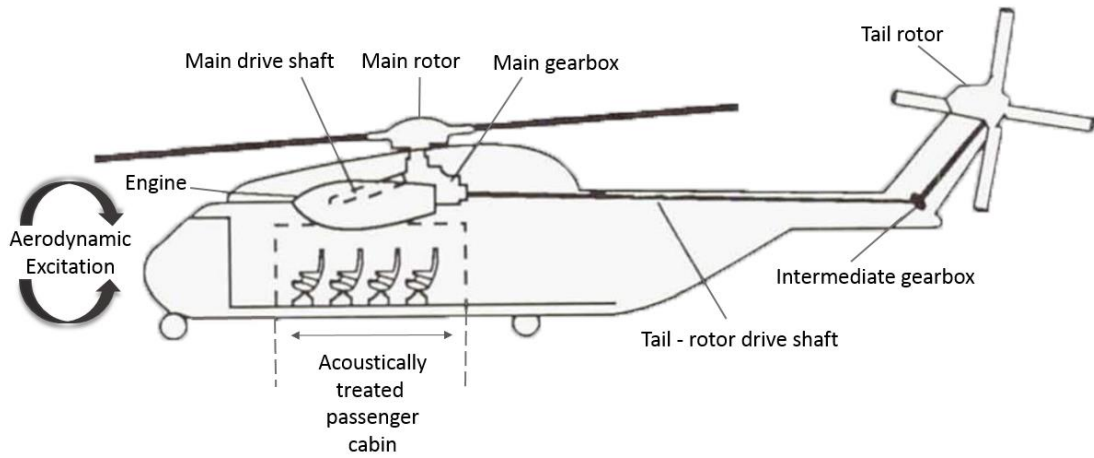


Figure 1.1 Main noise sources of helicopter

Travelling mechanism of sound through the air and the structure to the cabin interior must be well understood. The generating mechanism of noise in the helicopter cabin space can be categorized into two types; namely airborne noise and structure borne noise [4]. Structure borne noise contributes to low frequency content of the range, while airborne noise is responsible for high frequency content of the range. Acoustic pressure field is induced by structural vibrations travelling through the system components (Figure 1.2). On the other hand, panels excited by pressure waves and also acoustic leakages cause the pressure fluctuations into the cabin box as a representation of airborne noise in Figure 1.3.

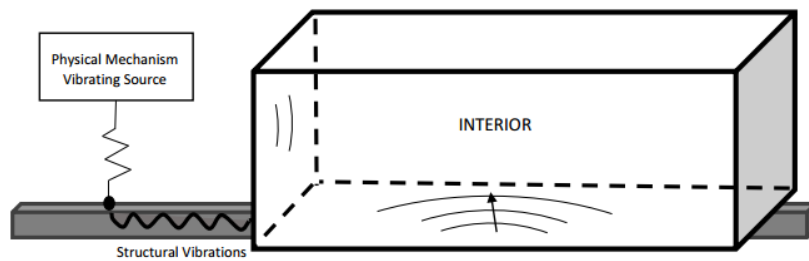


Figure 1.2 Structure-borne noise travelling mechanism

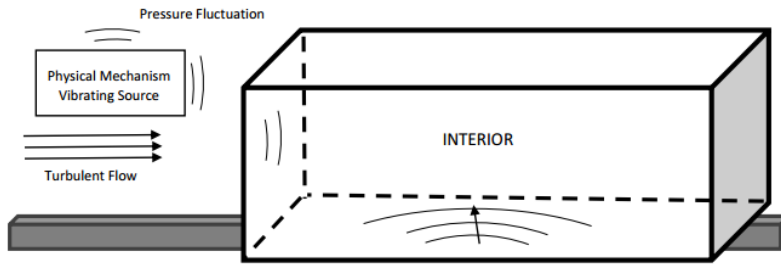


Figure 1.3 Airborne noise travelling mechanism

Excitations arisen from this multi-source environment propagate through the vibro-acoustic energy paths and reach up to passenger's ears as acoustic pressure. Specifically, primary sources with vibro-acoustic transfer paths for rotorcrafts are demonstrated in Figure 1.4 and Figure 1.5. Generally, the noise sources and receiver are fixed in the problem unless they are changed. However, the way that sound travels through could be modified by arranging structural parameters or adding acoustic treatments. Identification of the dominant sound travelling path comprises the difficult part of the problem.

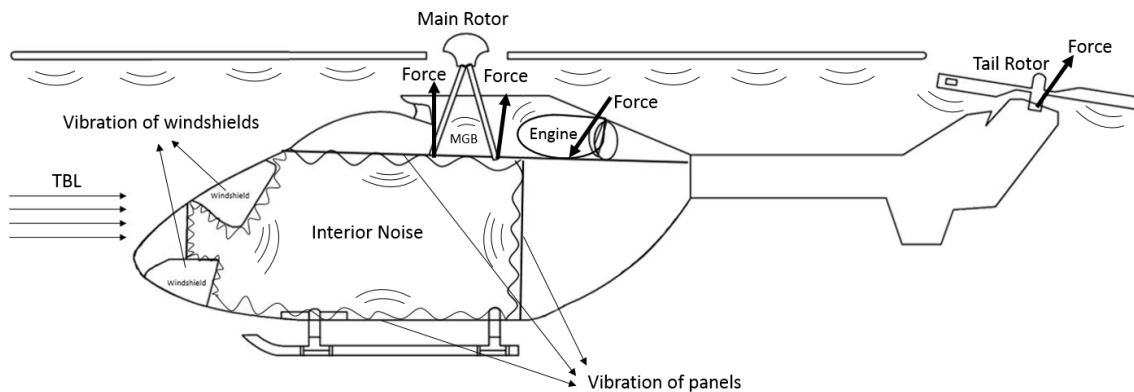


Figure 1.4 Airborne and structure-borne paths of helicopter noise [4]

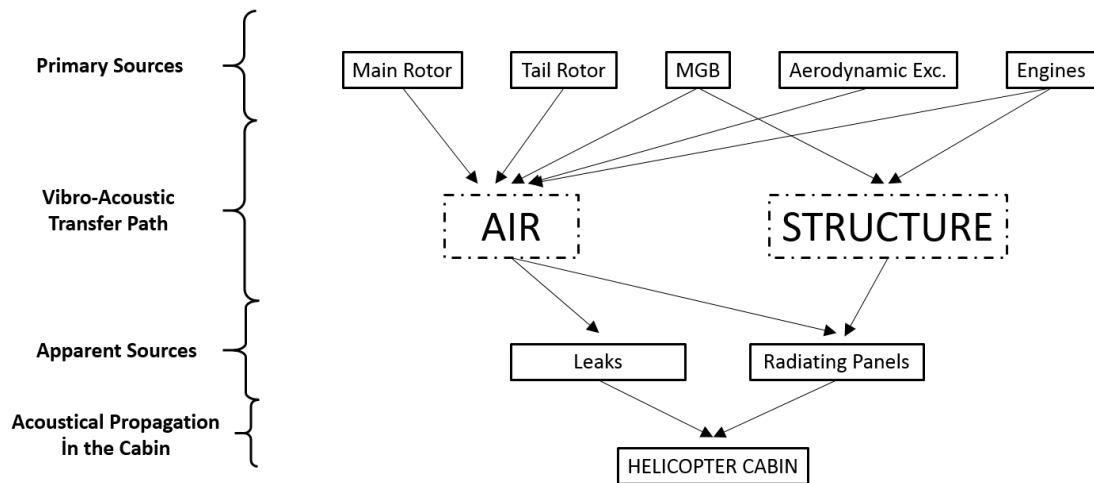


Figure 1.5 Noise travelling paths inside a helicopter cabin (Caillet, Marrot, Malburet, Carmona, 2005)

The acoustic spectrum of a helicopter in Figure 1.6 consists of broadband and discrete noises [5]. If the frequency range is separated into two sections, each section is dominated by different noise sources. Zooming low-medium frequency range, meshing frequencies of drive system and frequencies related to rotational speed of rotors and their first dominant harmonics cover low-medium frequency range from DC to 8 kHz. Beyond 8 kHz to 25 kHz, compressor and turbine blades of engine functions contribute due to high rotational speed of engine and their relative sidebands. It should be noted that the rotational speed of engine is about 100 times higher than that of rotors.

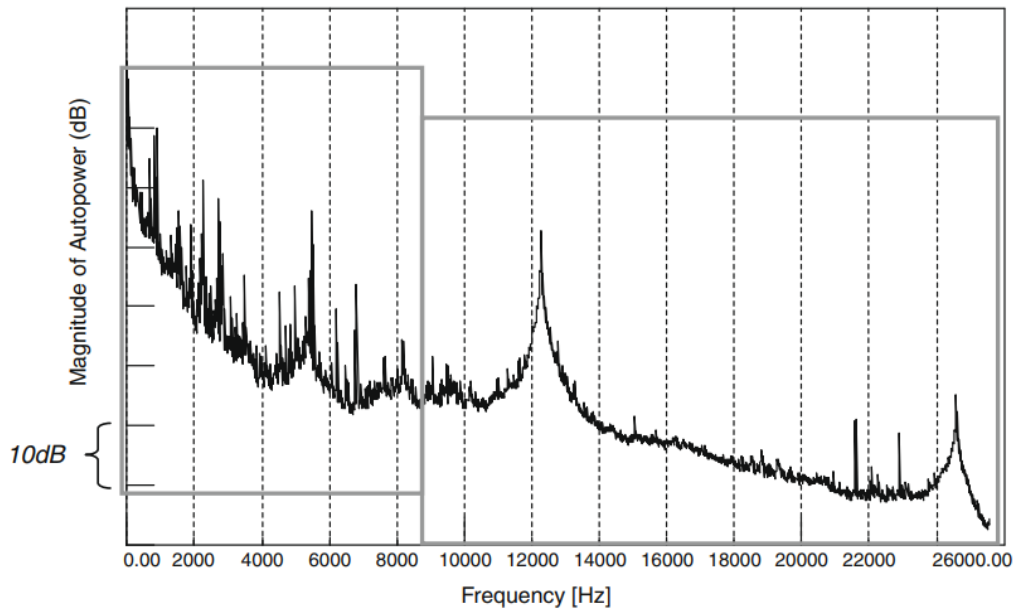


Figure 1.6 Noise characteristic of helicopter cabin (Mucchi, Pierro, Vecchio, 2005)

Generated noise from primary sources can be classified as mechanical and aerodynamic noise, as demonstrated in Figure 1.7 [6].

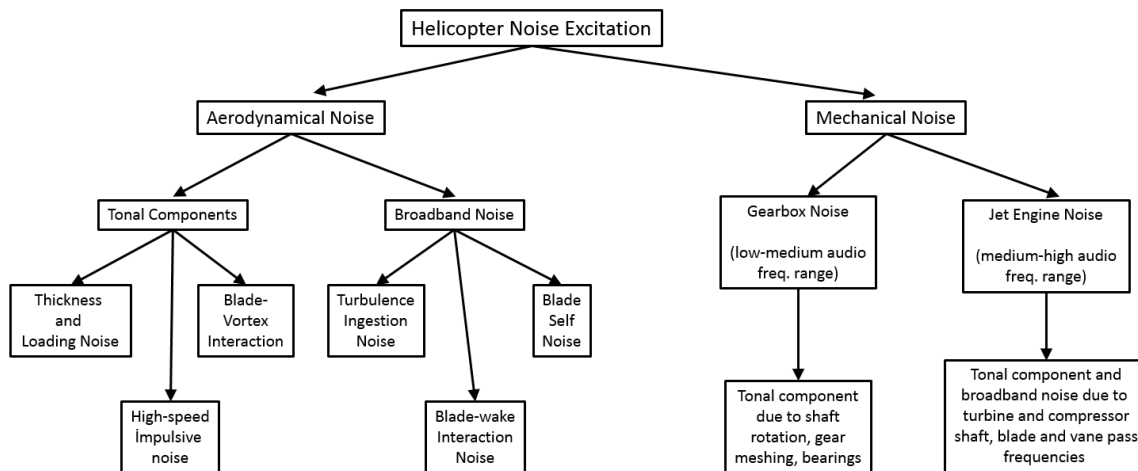


Figure 1.7 Noise classification of helicopter cabin (Mucchi, Vecchio, 2009)

The transmission and gear box noise is a pivotal contributor of helicopter's interior noise. Main gearbox system is an intermediate mechanical system to transfer power from engine to rotors [7]. Therefore, each gear rotates speedily and their interactions cause discrete tones in mid to high frequencies where human ear is sensitive. The mesh frequencies and their harmonics can be evaluated by multiplying the number of gear teeth with rotational speed of shaft. And also as mechanical noise, the blades inside the engine generate discrete noises in the high frequency range, 10-20 kHz while rotating at speed about 300,000 rpm.

Aerodynamic noise sources can be classified as tonal or broadband character. Main and tail rotor are the main generative aerodynamical sources in low frequencies ranging from 0 to 250 Hz. Such noises originate from rotation of rotors and their dominant harmonics. The blade vortex interaction known as one of the rotor noise type, and formed when a blade impacts a vortex created at the tip from a previous blade. This interaction cause a peak noise in the sound field which is in the low frequency range. Additionally, when the helicopter speed is relatively high, aerodynamic noise become dominant other than mechanical noises. It is arisen from pressure fluctuations over the body which impinge on the windshields and structures. Oscillations of structures generate sound pressures inside the helicopter cabin. Flow acts a loading on the flexible structures. Especially, at the high speed conditions, its effect is highly observable.

1.2. Methods for Helicopter Interior Noise Prediction

It is important to determine the most radiating panel and location of leaks to reduce the noise level to have quieter helicopter. Numerical and empirical methods are available to rank the contribution of each primary source upon helicopter cabin noise. Through these methodologies, one can estimate sound pressure variation thus acoustic energy distribution inside the helicopter cabin.

Helicopter interior noise prediction methodologies have been improved from year to year. Especially in the development phase of a new product, computer aided engineering is very useful to simulate the system response. Earlier, it is just done by performing an experiment, trial and error methodology, that causes late feedbacks to designers to improve. However, recently CAE tools could give an engineering assessment and a chance to guide the design before prototype testing period. Even if the simulation does not represent exactly the real-life conditions, the prediction accuracy is enough for initial evaluation. Finite Element Method, Boundary Element Method and Statistical Energy Analysis are the most studied ones for interior noise analysis [8]. There are many software covering up mentioned methodologies.

Finite Element Method and Boundary Element Method are deterministic approaches. In FEM, dynamic behavior of a structure or fluid is represented by differential equation of motion ensuring continuity. Initial and boundary-conditions with prescribed inputs are imposed into the model to solve the matrix derived from partial differential equations. Finally, acoustic pressures and displacements can be calculated through such an approach. The accuracy of the analysis is highly dependent on the size of mesh at high frequencies. For this reason, a structure or air is modelled with a great number of element to find the modes, especially the local ones that are effective for interior acoustic. FEM discretization is done for both surface and inside the body, whilst BEM discretization is of interest just surface or curve of a body [9]. For instance, interior cabin air can be represented either volume by using three dimensional finite elements or surface by using shell boundary elements. Through BEM, volumetric problems can be modelled as two dimensional surfaces. Thus, reduction of model, dimensionally one, is achieved. The formulation of theory is derived from integral equation of the displacement, Green's functions. The solution can be found numerically. BEM is highly accurate especially in the infinite and semi-infinite homogeneous domain [10]. The problem with complicated boundaries can be analyzed with BEM. In the literature, there are many studies in which FEM and BEM modelling and comparison are done.

The size of system equations of finite element model is dependent on number of degrees of freedom, affected by geometry and frequency range of interest. The variation of degree of freedom with respect to frequency and system volume is illustrated for fluid and structure domain in Figure 1.8, by P. Davidsson [11]. To avoid from local and global errors in the results, it is needed to have fine mesh resolution in Finite Element Method that results in long computational time. There can be million structural and acoustic modes for a typical car 3×10^6 and 1×10^6 , respectively, up to 10 kHz [11]. Considering long computational times and low accuracy of analysis, it is clear that FEM is not efficient in mid to high frequency range. Similarly, in BEM the system equations are difficult to solve even in a long time for high frequency range. The calculations are done for each frequency. Also, the results are inaccurate for high frequencies.

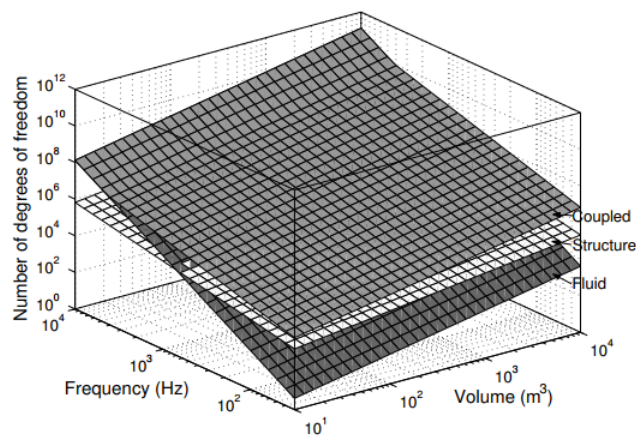


Figure 1.8 Relation between frequency and DOF in fluid and structural domain
(Davidsson, 2004) [11]

The weakness of classical numerical methods is that they are not presently unadapted for high frequencies. Statistical Energy Analysis is developed for the problems concerning mid-to-high frequencies. The difference between classical approaches and statistical

energy analysis lies in the physics behind the theories. FEM and BEM use variables such as force, displacement and pressure whereas SEA is energy based. The advantage of SEA is that it can be used in the early stage of design process since it does not need any detailed data to apply. It is well-suited method to pose the optimal design from the standpoint of acoustic. However, in the development phase, the power inputs could not be obtained. Therefore, it should be derived from the similar designs that already have overly information.

The complexity of a system is simplified by taking statistical average of a subsystem's properties in the model. Coarse design geometry with material, average spatial thickness, damping and absorption characteristic are enough to proceed for analysis. SEA model consists of a cluster of subsystems. They all are assigned with a statistical properties. The system is divided into portions called subsystems and each subsystem has its own modal energy and resistance that block energy transmission between one to another or energy coupling loss within their boundary. The number of subsystems in SEA model when compared to the number of elements in FEM model is extremely less. Therefore, one does not waste time in analysis process. SEA makes the calculations in terms of energy and gives the mean-averaged results for each subsystem. The effect of noise control treatments can be investigated easily by using SEA. The advantages and disadvantages of each method are displayed as a summary in Table 1.1.

Table 1.1 Comparison of simulation techniques

Limitations	SEA	FEM	BEM
Sensitivity to Small Parameters	Low Sensitivity	High Sensitivity	High Sensitivity
Computational Time	Short Time	Long Time	Long Time
Required Data	Coarse Data	Detailed Data	Detailed Data
Applicable Frequency Range	Mid to High Frequency	Low Frequency	Low to Mid Frequency
Cost of Computer Runs	Low-priced	High-priced	High-priced
Confidence of Prediction	Probabilistic	Deterministic	Deterministic
Spatial Response Distribution	Global Response	Local Response	Local Response
Applicable System Volume	Large Model	Small Model	Small Model

There are also hybrid methods which are combination of FEM and BEM or combination of SEA and FEM. Combination of different theories can be ideal solution for specific problems. Combining the advantages of each theory while removing disadvantages makes the hybrid methods ideal for some cases. By this way improvements on noise prediction are achieved.

Combination of SEA and FEM is kind of state of art vibro-acoustic analysis and most popular methodology. By use of such a hybrid model, predictions can be developed from models of noise and vibration across the full frequency spectrum. Local FE models can be added to SEA model to describe complex junctions and stiff components. Or, SEA of acoustic cavities or loads can be added to existing FE models. Hybrid coupling methods are generally used in mid frequency range termed as “twilight zone”. It extends existing SEA models to mid and low frequency range called as twilight zone.

1.3. Choice of Approach

The structural systems of a helicopter and the wide noise environment all together bring the complex model to set a well suited approach in the prediction process. As can be seen in the comparison, from Table 1.1, traditional methods are one step forward for some limitations. Yet, SEA left behind FEM and BEM providing simple and accurate results against the deficiencies of traditional ones. The classical techniques perform well in simple structures, but very limited success in complex systems.

It is simply concluded that rotary wing aircraft should be analyzed at different frequency intervals with different simulation methodologies. In general, it is preferred that full FEM model for low frequency, hybrid FEM-SEA model for mid frequency and SEA model for high frequency in the modelling of aircraft complex systems. Especially, FEM-SEA upskills the present SEA in structure borne-noise predictions. In frequency bands from 50 Hz to 20000 Hz, the selection of right approach based on the validity consideration makes the analysis easier, faster and more accurate. In this thesis, SEA and hybrid FEM-SEA models are constructed and the results are compared.

1.4. Motivations and Objectives

This study is a type of research about the noise field inside a helicopter. Properness of various prediction methodologies is investigated. Understanding main noise sources and analysis techniques with the associated theory behind is the key feature to progress throughout the evaluation. The main aim of this study is to develop a preliminary SEA model to predict the interior noise levels of a typical helicopter before the first flight. The SEA simulation procedure on a helicopter with a very limited data is achieved by producing two different models. The results, computational effort and cost are compared between the models. Further, the effect of application passive noise reduction treatments is also investigated.

CHAPTER 2

STATISTICAL ENERGY ANALYSIS

2.1. A Brief Introduction and Literature Survey

The basic theory of SEA is developed by R.H. Lyon in 1959 through examining two lightly coupled, linear resonators triggered by white noise sources [12]. The examination of power flow between the systems showed that it takes place from the resonator of higher vibrational energy to lower in proportion to energy difference between them. Meanwhile, Smith studied the response of a resonator to sound and proposed that the limit for the response is reached when the radiation damping is greater than mechanical damping of the resonator. Combining these two studies, Lyon and Maidanik [13] published a paper in which interaction of two oscillators with the extent of multimodal systems was investigated. Key points of SEA such as coupling parameter, modal damping coefficient and modal density were also emphasized in their study.

The basic theory of SEA was developed by using resonators as fundamental. The randomly excited systems are the situations that one can mostly encounter in SEA. The statistical model described with energy variables is the appropriate feature in SEA for random excitation. Potential and kinetic energy of the system can be written in terms of the peak amplitude of vibrational motion. In real world, structures are more complex though. Rather than a simple, lumped-parameter representation of dynamic system, the

physical properties are distributed over the structure. For these structures, the response can be represented as a group of independent modal resonators (Figure 2.1). In coupled resonators, the motion of resonator 2 is triggered by the force at resonator 1 or vice versa. Therefore, it can be seen the energy is shared between the resonators. If the coupling loss is greater than damping, the energies are equalized which is named “equipartition of energy”.

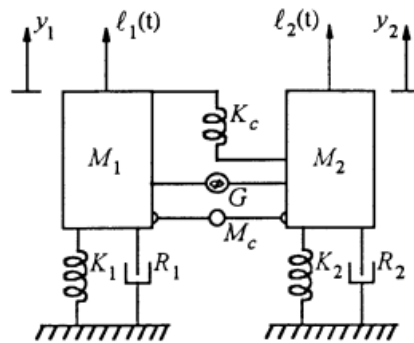


Figure 2.1 Linear resonators coupled by spring, mass, and gyroscopic elements (Lyon, 1995)

The examination of power flow from system 1 to system 2 shows [14];

- The flow occurs from the resonator of higher to lower vibrational energy in proportion to energy difference between them.
- Energy interaction is done by resonant frequencies dominantly rather than the other frequencies.
- The highest possible energy level of indirectly excited resonator is equal to the energy value of directly excited resonator. This occurs when the strength of coupling is higher than the damping of resonator 2.

In the survey by Fahy [15], the origin behind the theory was summarized. He explained details the reasons of the necessity of this alternative vibration analysis methods for high frequencies. The development of the theory was explained in a view of modal and wave approaches. Practical and theoretical advantages, beside deficiencies, of SEA was discussed. His work gives a general overview for the enquirers.

Applicability of SEA is an important issue on implementation of the theory for any problem and the modal density is one of the quantity. In a paper by Renji [16], it was indicated that the number of interacting modal pairs rather than the number of modes in each system is the key feature to represent the average power flow correctly. He prepared an experiment that resulted in whether measured and estimated values matches even if one of the subsystem has one mode in a frequency range. Agreement in the results despite the possible errors in the evaluation of the SEA parameter showed the presence of large number of modal pairs is sufficient to use SEA theory.

There are many studies to derive coupling loss factors by theoretically or experimentally. One was done by Langley in terms of space and frequency averaged Green functions between two directly coupled subsystems [17]. He also stated that the assumption of weak coupling does not assure zero value of coupling loss factor between subsystems that are not directly connected. General form of the equation was estimated based on both the wave and modal approaches.

The level of damping determines the strength of coupling between subsystems. Mace and Rosenberg [18] investigated that the behavior of two edge-coupled rectangular plates under the case of the light damping which is specifically called strong coupling and also of the high damping which is also named weak coupling. It was shown that subsystem irregularity is not important for weak coupling to obtain accurate predictions. They also calculated the coupling loss factor from FEA of plates with different geometries and the results are provided together with the values obtained from SEA wave approach.

Ribbed panels are largely used in many industrial applications. Maidanik [19] evaluated the response of reinforced panels by ribs to reverberant acoustic fields. The weight and

damping characteristic of the panel are increased by ribs. Despite the thought that heavier ribbed panel should vibrate with smaller mean square amplitude, experimental results showed that radiation ability of the ribbed panel is greater than the plane or unribbed ones. Theoretical formulation as a function of frequency was also studied and especially above 250 Hz, experiments and the theory were found to be in good agreement [19].

In complex structural-acoustic systems, there are a number of subsystems in which some missing information exists, which is difficult to model deterministically. Shorter and Langley [20] proposed a new method on wave concepts that enables inclusion of deterministic detail in the statistical SEA model which provides a solution to the mid frequency problem. Comparison between the wavelength and the dimension of the subsystem enabled discrimination of deterministic and statistical parts. The terminology with the theoretical combination of SEA-FEA methodology was presented in their paper. The total dynamic stiffness matrix of the model was the assembly of the dynamic stiffness matrix of deterministic subsystems and the direct field dynamic stiffness matrix of statistical subsystems. The basic difference between the traditional SEA and hybrid formulation is the determination of coupling loss factor which is named as power transfer coefficient in the hybrid methodology. The ensemble-averaged response is found by firstly solving the reverberant power balance equations. Then, the total energy response is given by the summation of the energies in direct and reverberant fields.

The hybrid method proposed by Shorter and Langley [20] was not extended to the coupling of statistical subsystems with acoustical components even though it was aimed to enable to model a component by deterministic or statistical method. For example, an area junction between a plate statistically modelled with a finite element cavity volume was not presented in their works. In 2008, Langley and Cordioli [21] extended the hybrid method to area junction which is the coupling over the field of the component rather than along the boundary.

The hybrid theory was validated by the study of Cotoni and others [22] with a structure. The experimental setup consisted of four thin panels bolted to a circular hollow beam

framework which was suspended from a corner and excited by a shaker. The acceleration response was obtained up to 1000 Hz applying a white noise signal to the system. Then, hybrid model of the test structure was constructed. The subsystems having long wavelength compared to the dimension of the subsystem was modelled with FE while the others with SEA. Direct field dynamic stiffness matrix was created to couple the FE model and SEA subsystems. When compared the estimated results of the analysis with measured ones up to 1000 Hz, it could be understood the performance of the method was sufficient.

The hybrid FE-SEA method with the modal type approach of hybrid coupling was introduced by Langley and Bremner [23]. This deterministic/SEA method was formed by using the principles of the theory of structural fuzzy for mid frequencies [24], Belyaev smooth function [25] and SEA. In their study, partitioning was achieved by setting a formulation for long wavelengths as named global while the other was local set. This separation could also be related to the modal density of a subsystem. Deterministic solution of the global set and SEA solution of the local set were the parts of the solution with due allowance for the coupling which exists between the two types of response. Through the analysis, the local mode response was found by SEA with the power input emanating from the presence of the global modes. Additionally, in this approach there was no need to find local response before the global response which makes the method direct rather than iterative.

The frequency range of the vibro-acoustic analysis generally extends up to 20000 Hz. A single methodology is not adequate for analysis of complex structures in such a wide frequency range. Accordingly, the effective mathematical modelling should be selected depending on frequency ranges. In the study of Millan [26], a typical satellite structure was analyzed by selecting a correct methodology at different frequencies. The criterion of choice was the modal density of subsystems which represent structural components. The procedure to apply the modal density criterion was formed by setting a critical modal count value which was 5 in their work. Subsystems were modelled with SEA if the number of modes was above 5. Else, FEM or BEM were used to model to related subsystems. Using FEM, BEM and SEA methods, ten different models were produced including

hybrid models. The results were validated with experimental results. Putting together the results of all models showed a smooth continuity.

2.2. Basis and Methodology of SEA

Statistical Energy Analysis is a method for studying diffusion of acoustic and vibration energy in a system. As a typical illustration in Figure 2.2, basic energy flow concept is showed for one of the coupled plates connected through one edge. Power balance equation for subsystem 1 can be derived in a simple form in Equation (2.1) and Equation (2.2) by applying energy conservation principle. The input power Π_{in} should be equal to Π_{out} for each subsystem.

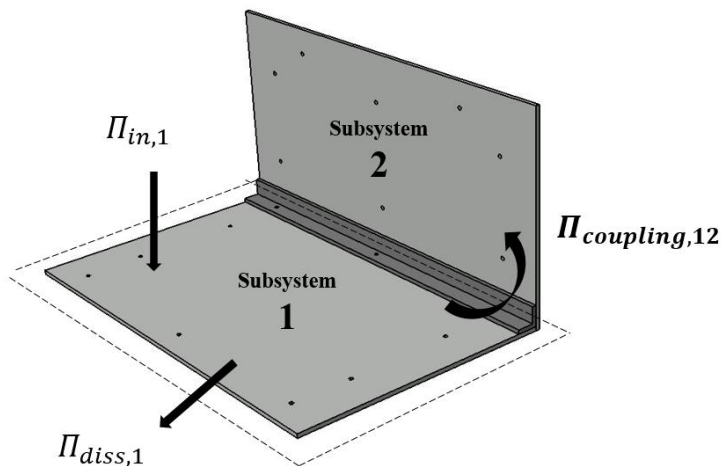


Figure 2.2 Simple illustration of coupled plates

$$\Pi_{in,1} = \Pi_{out,1} \quad 2.1$$

$$\Pi_{in,1} = \Pi_{diss,1} + \Pi_{coupling,12} \quad 2.2$$

The arrow leaving the system represents power lost which is defined as a ratio of energy dissipation within a material of subsystem with damping loss factor. The one pointing into the subsystem indicates external input power. Moreover, the arrow between the subsystems shows that there is an energy transmission between the subsystems that is determined by coupling loss factors which is the sharp end of the analysis.

High energy capacitive resonant modes in a dynamical systems are the main focus of SEA. In a frequency range, summation of all modal energies generates total modal energy level in a subsystem. For this reason, energy sharing between two different systems occurs in proportion to modal energy difference, not total energy. Mean square vibration velocity or acoustic pressure can be acquired from the steady state energy level after the analysis.

System with one energy degree of freedom per subsystem can be solved easily. In SEA, reduction of degree of freedom is so effective that set of energy balance equations may be solved by hand even if the system is relatively complex. It is not interested in exact solution for a specific point. Rather, time and space averaged solution is found.

SEA is simply a modelling procedure to estimate dynamical behavior of a system. The steps of SEA modelling are summarized roughly;

- Identify the model of a particular system
- Determine the parameters required
- Solve the power balance equations

2.2.1 SEA Subsystems

In the first part of the modelling process, the selection and size of participating structures into the model could be important. The integrity of subsystems into the dynamic model can have an impact on energy flow path. Modes acting as energy packages are the base elements in the analysis. The excitation of these modes triggers power flow between the subsystems. In the end, average value of the response can be obtained.

Subsystems are related with the physical elements which is a part of structure being modelled. Subsystems should exhibit similar dynamic behavior in itself and make up the system. The average and uniform distribution of similar modes through the subsystem are important while selecting the subsystems in a dynamic model. Each subsystem adds one energy degree of freedom to the model.

In SEA model, subsystems with different physical geometry and material characteristics are coupled and share the energy. Transmitted energy to another subsystem or outward from the system is determined by coupling loss factor and damping loss factor, respectively.

There are several ways to represent a dynamic system as a SEA model. It is preferred to model a system as simple as possible. As an example, interactions or losses may be evaluated as equivalent damping loss factor for simplicity.

SEA subsystem size should not be very big or small. Travelling waves should not decay through the subsystem which is the upper limit for the size of a subsystem. In the contrary, if the subsystem is coupled with a system, there is no need to set a lower limit for the size of a subsystem.

2.2.2 SEA Parameters

Three parameters are fundamental to determine level of response within an accuracy margin. This section is devoted to discuss the modal density, the internal damping loss factor and the coupling loss factor.

2.2.2.1 Modal Density

Modes of a subsystem represent potential energy capacity. For this reason, it should be counted in a frequency range. For complicated structures, it is hard to evaluate the mode count. It can be assumed the sum of modes of each component. Another procedure to determine the mode count of subsystems is the measuring frequency response function which should be done more than one to minimize the error in results. In theoretical evaluations the modal density is the most used form of calculating the mode count. Modal densities for simple geometries and the formulas are outlined below:

The formula derivation is mostly dependent on geometry and boundary conditions. One dimensional subsystem with length L which is much greater than its cross-section has different mode shapes and wavelengths. The wavelength of N^{th} mode is given by

$$\lambda_N = \frac{2L}{N \pm \delta_{BC}} \quad 2.3$$

where δ_{BC} is a constant depends on boundary conditions and usually corresponds to less or equal to 1 [12]. The related wave number per unit length is,

$$k_N = (N \pm \delta_{BC}) \frac{\pi}{L} \quad 2.4$$

In the mode count equation below, the mode with a particular wavenumber can be found by,

$$N(k)^{1D} = \frac{kL}{\pi} \pm \delta_{BC} \quad 2.5$$

Considering the wavenumber is dependent on frequency due to dispersion relation $k = k(\omega)$, the differentiation of N with respect to ω gives the modal density $n(\omega)$ of a subsystem,

$$n(\omega)^{1D} = \frac{dN}{d\omega} = \frac{L}{\pi c_g} \quad 2.6$$

where c_g is the group speed of a wave.

The generalized modal density equation for a simple rectangular geometry as a two dimensional system with small thickness compared to a wavelength is defined as,

$$n(\omega)^{2D} = \frac{A\omega}{2\pi c_\phi c_g} + \Gamma'_{BC} P \quad 2.7$$

where quantity Γ'_{BC} can be assumed zero and P is the perimeter which is less critical as the frequency increases. Additionally, A is the area of the system, c_ϕ and c_g are group and phase velocities, respectively.

Finally, the modal density of a fluid in a system of V volume that is surrounded by walls can be found by;

$$n(\omega)_0^{3D} = \frac{V\omega^2}{2\pi^2 c_0^3} + \frac{A\omega}{8\pi^2 c_0^2} + \frac{P}{16\pi c_0} \quad 2.8$$

2.2.2.2 Damping Loss Factor

The parameter that specifies the damping loss for a subsystem can be evaluated by theoretically or experimentally. The overall response and damping loss factor has an inverse ratio and it can be written by definition,

$$\eta = \frac{E_{diss}}{2\pi E_{tot}} \quad 2.9$$

Most metals have small damping values. Energy is dissipated at each frequency, f (Hz). However, it affects the response level especially at high frequencies. Some of the energy may be converted into heat or dissipated by friction.

Evaluation of damping loss factor can be done experimentally since theoretical or empirical methods may not be applicable for a specific subsystem geometry. There exist three popular experimental procedures to determine the damping loss factor; the decay rate, the half-power bandwidth and power balance method. It should be noted that there are limitations and errors in measurement due to complex behavior of damping.

In decay rate method, the experimental setup consists of a system with a continuous excitation and equipment for displaying response of the system in time. A very sudden shut off of the excitation source causes the decay in response. The decay rate in units of dB/sec is used for the calculation of damping loss factor for a single resonant mode as,

$$\eta = \frac{DR}{27.3f} \quad 2.10$$

The response also can be plotted as linear amplitude. In this approach, damping loss factor can be evaluated as,

$$\eta = \frac{0.22}{fT_{1/2}} \quad 2.11$$

where $T_{1/2}$ is a measure of decay that is equivalent to time required to reach the half-amplitude response. Also, in the case of room acoustics, the damping is calculated by the reverberation time T_R defining the time taken for the energy to decay by 60 dB after a noise source has been switched off [12].

$$\eta = \frac{2.2}{fT_R} \quad 2.12$$

In modal bandwidth method, the experimental setup consists of a system with power input and equipment for displaying response of the system in frequency. The damping value of a single mode can be calculated by,

$$\eta = \frac{\Delta f}{f_n} \quad 2.13$$

where f_n is the resonance frequency and Δf is the half-power bandwidth that is the spacing between the two points of modal frequency response function which has 3 dB less magnitude than the peak level.

The damping factor can also be calculated from the power balance method by measuring input power and total response energy at steady state,

$$\eta = \frac{\Pi_{in}}{2\pi fE_{tot}} \quad 2.14$$

2.2.2.3 Coupling Loss Factor

The power transfer from the subsystem with high modal energy to the low one is proportional with coupling loss factor. The power flow can be formulated as,

$$\Pi_{12} = 2\pi f(\eta_{12}E_1 - \eta_{21}E_2) \quad 2.15$$

where η_{12} and η_{21} represent the coupling loss factors between the subsystems. Also, E_1 and E_2 are the total energy of subsystem 1 and 2. There exists reciprocal relation between CLF's which mostly makes the SEA calculation easy. In the Equation (2.16), $n(\omega)$ represents the modal density of each subsystem.

$$n(\omega)_1\eta_{12} = n(\omega)_2\eta_{21} \quad 2.16$$

Alongside of experimental procedures and numerical methods, CLF expression could be obtained by wave approach or modal approach, theoretically. Although similar results are obtained by both formulations, the modal approach involves with difficulties like calculation of complicated integrals. Additionally, there exist many theoretical works available in literature for wave approach. For these reasons, the wave approach is preferred.

Calculation of CLF is highly dependent on the type connection as point, line or area contact between the pairs. Point junction can be created by the connection of two one-dimensional subsystems. Some of the incident energy in subsystem 1 is transmitted, some is reflected as shown in Figure 2.3. The energy of subsystem 1 at the junction is the total energy of incident and reflected wave since transmitted energy into the subsystem 2 is assumed to be not have any contribution to the reverberant field at the junction.

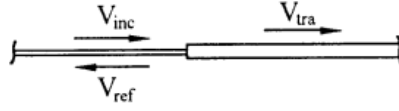


Figure 2.3 Wave approach to coupling of 1D elements (Lyon, 1995)

The basic formula of this transmitted power is;

$$\Pi_{12} = 2\pi f \eta_{12} E_1 \quad 2.17$$

Also, it can be formulated based on wave transmission model as;

$$\Pi_{tra} = \tau_{12} \Pi_{inc} \quad 2.18$$

where τ_{12} is the transmission coefficient that is evaluated with complex and real part of the infinite system impedances of two subsystems as,

$$\tau_{12} = \frac{4R_{1\infty}R_{2\infty}}{|Z_{1\infty} + Z_{2\infty}|^2} \quad 2.19$$

The reflected power can be calculated as,

$$\Pi_{ref} = |r|^2 \Pi_{inc} \quad 2.20$$

where $|r|^2 = 1 - \tau_{12}$. Now one can evaluate the total dynamical energy of subsystem 1 with L_1 , length of subsystem 1 and c_{g1} as group speed,

$$E_1 = \frac{L_1}{c_{g1}} (\Pi_{inc} + \Pi_{ref}) \quad 2.21$$

From Equation (2.17) and Equation (2.18), CLF can be found as,

$$\eta_{12} = \frac{\overline{\delta f_1}}{\pi f} \frac{\tau_{12}}{2 - \tau_{12}} \quad 2.22$$

Likewise, two plates connected through one edge form a line junction in simple form. Similar to point connection, some of the incident energy with an angle θ from normal in subsystem 1 is transmitted, some is reflected as shown in Figure 2.4. Note that the incoming power $L_j \cos(\theta)$ times the power per unit width in the wave.

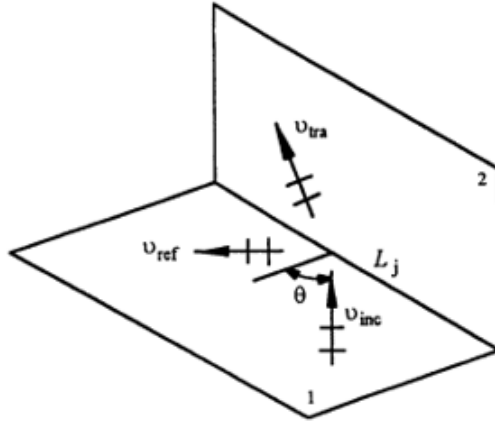


Figure 2.4 Wave analysis of a line junction (Lyon, 1995)

The value of coupling loss factor changes with the angle of incidence and can be calculated with the following function,

$$\eta_{12}(\theta) = \frac{c_{g1} L_j \cos(\theta)}{\omega A_1} \frac{\tau_{12}(\theta)}{2 - \tau_{12}(\theta)} \quad 2.23$$

where τ_{12} is transmitted coefficient, A_1 is surface area and c_{g1} is group speed.

The interaction of a pair of three dimensional subsystems creates area junction, A_j . The value of an area coupling factor could be determined by the formula,

$$\eta_{12}(\theta) = \frac{c_{g1} A_j \cos(\theta)}{\omega V_1} \frac{\tau_{12}(\theta)}{2 - \tau_{12}(\theta)} \quad 2.24$$

θ is angle of incidence, c_{g1} is group speed, V_1 is volume of the three dimensional subsystem and τ_{12} is transmission coefficient. Note that the incident power is $A_j \cos(\theta)$ times the power per unit area in the wave.

2.2.3 Power Balance Equations

The power inputs to SEA model can be found from analytical expressions or experimental measurements as well as the SEA parameters. The parameter is important since there is a relation between the response predictions and the power inputs. They are proportional that implies any change in power affects the response in same way.

In SEA, the generalized forms of the sources are as force, pressure or motion. For the structures, time averaged product of the force and the velocity gives the power as a point excitation. This power is calculated for acoustic spaces with the time averaged product of the volume velocity and the pressure. The expressions for the power input can be formulated below:

$$\Pi_{in} = \langle l v \rangle = \langle l^2 \rangle G_{in} = \langle v^2 \rangle R_{in} \quad 2.25$$

$$\Pi_{in} = \langle U p \rangle = \langle U^2 \rangle R_0 = \langle v^2 \rangle G_0 \quad 2.26$$

Sometimes, the system is excited over a distributed area. In such cases, the input power depends on the matching activity of the spatial pattern of the excitation with the system mode shapes. It is mostly preferable to calculate the power input to a subsystem coupled with another by using coupling theory. One of typical example is the turbulent boundary layer TBL source over the body, which excites the bending modes of the related plate.

The flow equation using the SEA parameters for each subsystem can be written in matrix form. Then it is solved to obtain the average modal energies of subsystems. The modal energy can be converted to the dynamical variables.

Bringing all the power balance equations into matrix form, it can be written as,

$$[B]\{\phi\} = \{\Pi_m\} \quad 2.27$$

B matrix is symmetric, positive definite and diagonally dominant. Therefore, inversion of matrix can be done easily. For these reasons, B matrix facilitate the calculation by decreasing computational effort. The response can be found by solving familiar linear algebra equation,

$$\{\phi\} = [B]^{-1} \{\Pi_m\} \quad 2.28$$

Upon solution of the power balance equations, modal energies for subsystems can be found. This quantity of interest is the primary response, however, generally pressure or acceleration is preferred to assess the results.

The mean energy can be converted to velocity variable. In Equation (2.29), M is the uniformly distributed mass and v is the mean square velocity.

$$E = M \langle v^2 \rangle \quad 2.29$$

The velocity level can be described by the logarithmic or dB scale equation with the reference level $v_{ref} = 10^{-9}$ m/s.

$$L_v = 10 \log(v_{rms}^2 / v_{ref}^2) \quad 2.30$$

For acoustic subsystem, energy and pressure is related by,

$$E = V \langle p^2 \rangle / \rho c^2 \quad 2.31$$

where ρc is the characteristic impedance of the subsystem and V is the volume of the subsystem. Since the order of energy in magnitude changes excessively, sound pressure level in decibel scale is defined as,

$$L_p = 10 \log_{10}(p_{rms}^2 / p_{ref}^2) \quad 2.32$$

where p_{ref} is $20 \mu Pa$ for acoustical systems.

2.3 Basis and Methodology of FEM-SEA Hybrid Method

Hybrid method is used for the analysis of complex systems in which uncertainties exist in some subsystems. Power balance equation are incorporated with dynamic equilibrium equation to form a hybrid theory. The main difference between the classical SEA and hybrid FE-SEA equations lies in the calculation of the coupling loss factor [27].

A system model can be formed as deterministic and statistical subsystems with different boundaries as indicated in Figure 2.5. An excitation causes diffuse reverberant field in a subsystem. This energy is transmitted to direct field of another one. In the hybrid method, it is not needed to model entire systems with deterministic methods. The modeling type

of the subsystems is chosen by their dynamic behavior while random or deterministic boundaries are defined according the information level about the boundaries. The junction can provide a connection between two statistical subsystems, two deterministic subsystems or one statistical and one deterministic subsystems.

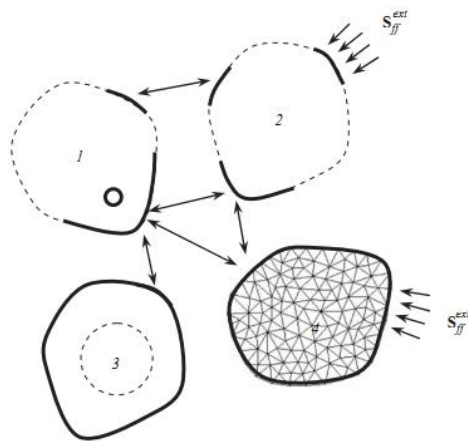


Figure 2.5 Schematic representation of hybrid system (Shorter, Langley, 2005)

The response of the system is described by a number of degrees of freedom in hybrid model. It is represented as q_1 for deterministic subsystems and hybrid connections while as q_2 for the junctions of statistical subsystems. The total degrees of freedom of the system to represent displacement responses can be defined as combination of q_1 and q_2 .

$$q = [q_1^T \ q_2^T]^T \quad 2.33$$

When a force, f_d , is exerted onto the deterministic subsystem, its motion can be written by an equation,

$$D_d q = f_d \quad 2.34$$

D_d represents the dynamic stiffness matrix of deterministic subsystems at frequency, ω . It can also be written for the statistical ones however the presence of uncertainty forms the problem to describe it exactly. Therefore, the dynamic behavior should be described with statistical description. The contribution of direct field and reverberant field of a statistical subsystem constitute in its total response. The uncoupled equation of motion is defined by,

$$D_{dir}^{(m)} q = f + f_{rev}^{(m)} \quad 2.35$$

where direct field dynamic stiffness matrix, D_{dir} , represents the force at the junction region. The right side of the equation is comprised with vector of generalized forces, f and the blocked reverberant force on the connection, f_{rev} .

Combining Equation (2.34) and Equation (2.35),

$$D_{tot} q = f_{ext} + \sum_m f_{rev}^{(m)} \quad 2.36$$

where

$$D_{tot} = D_d + \sum_m D_{dir}^{(m)} \quad 2.37$$

The average response, q , with uncertain boundaries in cross spectral form is given in Equation (2.38). In this equation, α_m is a value related with power input of reverberant field.

$$\langle S_{qq} \rangle = D_{tot}^{-1} \left(S_{ff}^{ext} + \sum_m \alpha_m \text{Im} \{ D_{dir}^m \} \right) D_{tot}^{-H} \quad 2.38$$

with $\alpha_m = \frac{4E_m}{\pi\omega n_m}$ where E_m is the total energy of m^{th} subsystem and n_m is its modal density. To find total energy of each statistical subsystem, the power balance equation should be solved for reverberant fields;

$$\left(M_m + h_{tot,m} \right) \frac{E_m}{n_m} - \sum_n h_{mn} \frac{E_n}{n_n} = P_{in,0}^{(m)} \quad 2.39$$

where

$$P_{in,0}^{(m)} = \frac{\omega}{2} \sum_{jk} \text{Im} \{ D_{dir,jk}^{(m)} \} (D_{tot}^{-1} S_{ff}^{ext} D_{tot}^{-H})_{jk} \quad 2.40$$

$$h_{mn} = \frac{2}{\pi} \sum_{jk} \text{Im} \{ D_{dir,jk}^{(m)} \} (D_{tot}^{-1} \text{Im} \{ D_{dir}^{(n)} \} D_{tot}^{-H})_{jk} \quad 2.41$$

$$h_{tot,m} = \frac{2}{\pi} \sum_{jk} \text{Im} \{ D_{tot,jk}^{(m)} \} (D_{tot}^{-1} \text{Im} \{ D_{dir}^{(m)} \} D_{tot}^{-H})_{jk} \quad 2.42$$

$$M_m = \omega n_m \eta_m \quad 2.43$$

The coefficient h_{mn} is a kind of coupling loss factor in hybrid theory. $h_{tot,m}$ is the outgoing total energy of m^{th} reverberant field. Also, M_m represents the modal overlap factor.

CHAPTER 3

APPLICATION OF SEA METHOD

3.1 Aircraft Based Applications of SEA

In the preliminary phase of design, SEA method is usually chosen to predict noise characteristics of a craft to save both time and cost in the development process. Perazzolo and Costa [28] constructed the confident vibro-acoustic model of AW139 helicopter with 1068 SEA subsystems before the first flight. In the model, structural damping was identified from the test samples while cavity absorption was determined from the measured reverberation time. First part of the work covered the analysis with unitary loads in the frequency range from 250 to 10000 Hz. The results showed that the cabin roof was the main energy path to the receiving cavity, especially at 2000 Hz. After the model validation, different trim configurations were applied to the model with acoustic materials. Efficiencies of the treatments were then comparatively evaluated concerning weight. The study was pointed out that SEA simulation is very useful to rank the contribution of each source even if there is lack of information.

Another study done by Kiremitçi [29] is to predict noise characteristics of a craft even if the design is not finalized. Before the critical design phase of the aircraft project, the interior and exterior acoustic signature of a trainer aircraft was examined with two different models in his study. One was created by 28 SEA subsystems with 116 junctions.

The wing and empennage parts were excluded from the first model since their contribution was not significant inside the cabin. The other model was FE/SEA hybrid model including FE parts into the complete SEA model. Determination of the FE structural subsystems was done by modal density evaluation. The input excitations, propeller noise and TBL noise, were applied to both models with different structural damping values and the results were compared.

Curved panels with ribs are the customary structures for helicopters. Perazzolo and Cenedese [30] validated the SEA model of rib panels by identifying the construction as singly curved shell with material parameters. Meantime, a FEA model of this single component was developed. Comparison was done by counting number of modes in 1/3 octave bands, which results in good harmony between two models except some discrepancies at low frequencies. In the second part of the work, A109 helicopter was simulated with 434 structural and 33 acoustical SEA subsystems. Large and small holes of some structures were also presented in the SEA model to represent acoustic leakage to the cabin cavity. Whilst validation process, trend of the predicted sound pressure levels throughout the frequency range differed from the measured ones. It was indicated that the impedances of the subsystems were the reason for this discrepancy since they were used to extract the dynamical loads. Then, the subsystem parameters were changed to have the same impedances with the experimental ones. The compliance was obtained between the acoustic responses in the second analysis.

There are many different techniques to represent a structure while modeling with SEA. Cordioli and Gerges built a vibro-acoustic model [31] with two different subsystem definitions of double wall construction of EMBRAER aircraft. One of them simplified the structure not modeling interior panels as subsystems. They were included in the model in the form of additional damping. The other one named as explicit method included the interior panels as SEA subsystems. Although the model became complicated with explicit method, it allowed the analysis of detailed parts like vibration isolators. On the other hand, a good agreement between the two techniques indicated the implicit method was more

effective than the other in a way of simplicity and time spending during model development.

In the prediction of interior noise using SEA, it is generally hard to obtain acoustic power inputs. Butts [5] from Sikorsky Aircraft Corporation calculated the input source levels by the method of weighted least squares using test data of a similar helicopter. He modelled the helicopter consisting of aircraft skin with the frames and longerons and also cavities. The focusing point of his study was to determine the location of inputs with derived source levels. The power inputs of main and tail rotors were located at the external cavities while the gearbox noise input was applied to the cavities between longerons and frames which is the region of main gear box attachments. Results for SEA power inputs were found by applying weighted least squares method to flight test data and transfer matrix which was created from unit resultants at 1 watt for each source type.

The experimental SEA study was carried out by Bonilha and Han [32] to predict dynamic characteristic and response of S-92 helicopter sidewall section which is made of airframe, trim panels and also some acoustical materials. In the course of model development, some SEA parameters were found by experimentally for all individual structures. The Lalor equation [33] was used to evaluate coupling loss factors by transfer functions obtained from the system excited by a hammer. Moreover, the damping loss factor was computed measuring decay rate of the response of the excited system. The CLFs were also theoretically calculated by the approach named as line wave impedance [34]. In this approach, a junction was idealized by a series of strip plates and transmission coefficients were obtained to determine coupling factor along a line. Since the results from the formulation was compatible with the values gathered in the experiment, they were used as inputs in the SEA model.

The term “ mid frequency problem” is the most encountered problem for vibro-acoustic analysis, especially in complex structures with components displaying different wave characteristics. Cordioli [35] stated that the advisable frequency limit is 250 Hz for deterministic modeling in terms of computational time and sensitivity rather than

statistical SEA which is widely used beyond 300 Hz. He also stated that structure-borne transmission is analyzed with FE better while the analysis with airborne noise sources is usually done with SEA. Consequently, the hybrid FE-SEA model of a full vehicle was constructed to predict vibrational response of some structures and acoustical response of interior cavity from the 200 Hz to 1000 Hz. In the beginning of hybrid modeling, a simple methodology based on modal analysis and forced response analysis was used to verify the subsystem partitioning as SEA or FE. Structures containing more than 3 modes per frequency band were selected as SEA subsystems. SEA parameters for simple geometries were calculated from analytical formulations. On the other hand, they were determined from local FE models for complex geometries. In the validation part, half vehicle FE model with number of 330,000 nodes was created. Solution time was about 12 hours of FE model and this time was around 25 minutes for hybrid model with 165,000 nodes in the model.

Applications of SEA extensions for complicated structures were also studied by Cotoni in [36]. Three different advanced models were constructed to improve the prediction of aircraft interior noise. All analyses were done for mid frequencies up to 1600 Hz. The first model was a hybrid model of bin-frame-tie rod assembly excited with a point force at the end of tie rod. Two singly-curved shell SEA subsystems were combined with a FE model of frame with 3783 nodes. Connections between the beam and frame were represented by hybrid point junctions. In the second portion of the paper, skin-stringer-frame construction excited by different unitary loading was modelled with full SEA and also FE-SEA hybrid method. Periodic formulation of SEA was used to model sidewall ribbed panels. The two SEA floor panel with FE stiff floor beams were the rest of the advanced hybrid model. Hybrid line junctions were created between the SEA subsystems and FE subsystem. Experimental results were in agreement with the hybrid predictions above 200 Hz. The low number of beam modes, which was defined in the paper as less than 3 modes per frequency band was the reason of inconsistency below 200 Hz. It was demonstrated that even if computational time is shorter for hybrid solutions, more effort is needed to

construct the model. As a third model, Boeing 737 section panel was modelled by adding more details with FE on rubber mounts at the connection of sidewall and trim panels.

3.2 General Overview of Simulated Rotorcraft

In this study, Turkish Light Utility Helicopter (TLUH) is modelled as a practical application of the theory. TLUH development program was signed between Turkish Aerospace Industry (TAI) and Undersecretariat for Defense Industries on September 26, 2013. Program has started on June 15, 2016. The scope of Turkish Light Utility Helicopter Program is to design, develop, implement, integrate, test, certify and qualify a 5 ton class light utility helicopter which will have civilian and military variants. TLUH is a conventional type helicopter with two rotor systems, one main rotor and one tail rotor. General view of helicopter is presented in Figure 3.1.



Figure 3.1 General view of Turkish Light Utility Helicopter

The overall helicopter length is 14 meters and the width of the tail section is 3.9 meters. The span of the main rotor is 13.2 meters. TLUH is capable of carrying total 12 persons including, 1 pilot, 1 co-pilot side by side, 1 crew chief and 9 passengers. The cabin design was specified depending on the reviews between human factor engineering, crashworthiness strategy and the seat manufacturers. The dimensions of the current cabin are given in Table 3.1.

Table 3.1 Cabin dimensions

DIMENSION	VALUE (m)
Cabin width	2.08
Cabin length	2.54
Cabin height	1.37

Main characteristics of TLUH are given in Table 3.2 below.

Table 3.2 Main characteristics of TLUH

Maximum Take-off Weight	6050 kg
Number of Main Rotor Blades	5
Rotational Speed of Main Rotor	313.66 rpm
Number of Tail Rotor Blades	4
Rotational Speed of Tail Rotor	1497 rpm
Design Limit Speed	165 knots

3.3 Modeling Process

For the purpose of determining interior cabin noise levels, a SEA model must be properly constructed. In this section, two different models are demonstrated to predict cabin noise level of TLUH in an extensive frequency range with reference to methods summarized in Chapter 1. One approach involves SEA where structures are modelled by SEA methodology while the other approach is hybrid FEM-SEA where stiffer components are constructed with finite element while the rest represented by SEA subsystems. The vibro-acoustic analysis is performed from 125 Hz to 16000 Hz by VA One Software 2016 developed by ESI Group.

3.3.1 SEA Model

The first step of the modeling in the SEA methodology is to identify subsystems. The fundamental modeling elements are a family of structural and acoustic subsystems. There are numerous components and noise paths around the helicopter cabin cavity which is the part known to be most sensitive to noise. The model should be simulated representing all the related body panels and their internal and external interactions. Therefore, the whole helicopter structures are examined and broken up into regions except the cowling, firewall and fairings, assuming no constitutively acoustic contribution inside the helicopter cabin. The finite element model of the helicopter structures is assisted in the definition of the subsystem division. The SEA subsystems are developed from imported FE data provided in Figure 3.2.



Figure 3.2 Imported finite element model of TLUH

The division of the structures is done based on the actual material difference between the components. As a typical aerospace structure, helicopter consist of mostly aluminum sheet metals, a few sandwich panels, composites and rib stiffened plates. Based on the design choice and locality of the panels, the materials might be isotropic aluminum, composite or metallic skin reinforced by stiffeners. Also, optior and polycarbonate as window materials exist. It is generally not necessary to provide much detail when modeling a subsystem. However, the energy storage capacity of each subsystem should be as close as possible to those of the physical components. Therefore, the mode number for each frequency band, mass density and space-averaged stiffness of each subsystem should also have approximately the same value with the physical components. The complexity of the helicopter structures is simplified by considering uniform distribution of dominant material in terms of dynamic properties. It is just required to assign the overall physical characteristic by an approximate estimate of properties. It is important to check that assignment of material parameters is correctly done. The constructed SEA model is presented in Figure 3.3. Different subsystems are denoted with different colors and names.

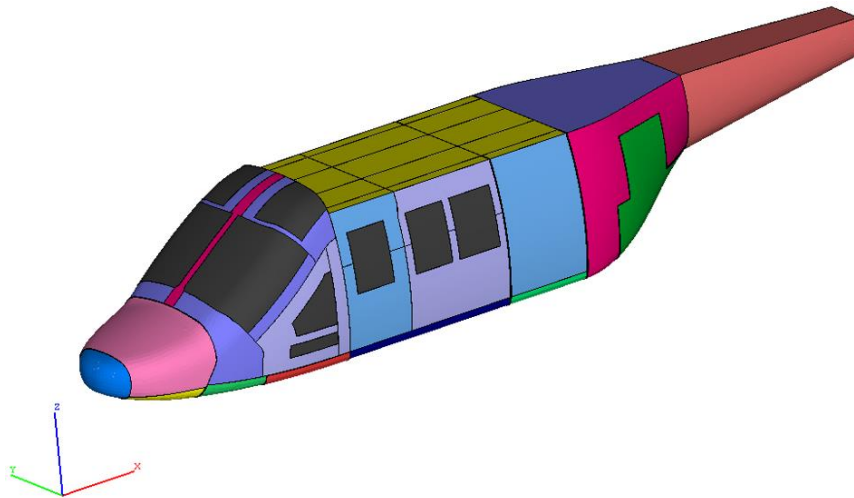


Figure 3.3 Complete SEA model of TLUH

The existence of the exterior acoustic space are also modelled by adding external acoustic cavities and Semi-Infinite Fluids (SIF) shown in Figure 3.4. These subsystems and creation of SIFs provide the sound propagation around the helicopter to outside.

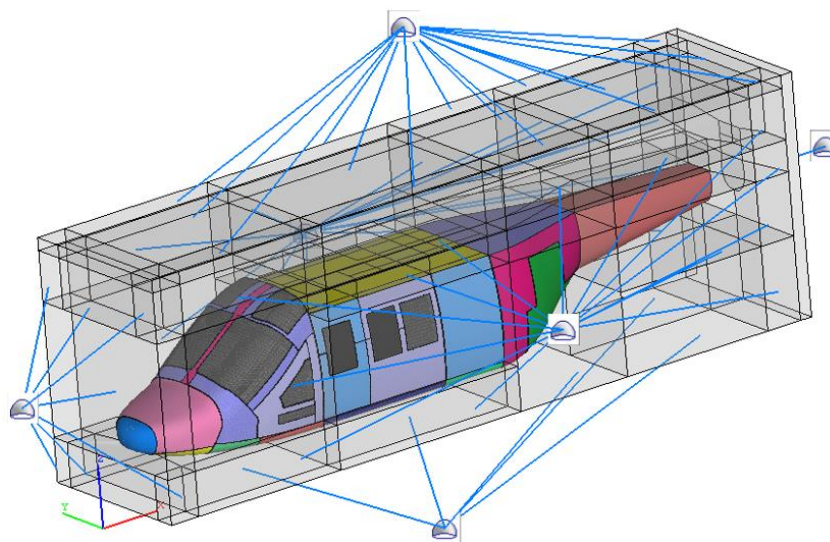
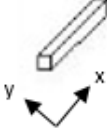


Figure 3.4 SEA Model with exterior acoustic space

There exist 185 SEA subsystems (101 structural, 84 acoustical) in the developed model. The subsystems are constructed based on foresight of source-path-receiver locations. In the library of VA One software [37], subsystems could be defined as a flat plate, single-curved shell, cylindrical shell and double-curved shell in agreement with geometrical shape of the aerodynamic surfaces. According the panel curvature, the selection of the subsystem from the library can be done. Volumes inside and outside the helicopter are defined as an acoustical SEA subsystem. Different subsystems support different wave fields, as tabulated in Table 3.3 [38]. Calculations are done for each wave field types. There are three distinct groups of resonant modes to determine the statistical energy level for SEA plates or shells subsystems. Bending modes correspond transverse wave fields where in-plane modes correspond extensional and shear wave fields. Transverse flexure resonant modes carry the most energy and excite the acoustic cavities. A scalar pressure wave field is used to characterize an acoustic cavity.

Energy transfer and the connectivity between the subsystems are covered by junctions. There are 670 (130-point junctions, 206-line junctions, 334-area junctions) junctions in total in the model. Junctions are located between the subsystems with different energy levels so that an amount of power leaks from one subsystem to the other. Junctions connect the subsystems and could be produced manually or by automated feature of VA One software.

Table 3.3 Wave fields of SEA subsystems

Subsystem	Wave field	SEA Idealization
Beam	Bending I_{xx} , Bending I_{yy} Torsion, Extension	
Flat Plate	Transverse Bending In-plane Extension In-plane Shear	
Singly Curved Shell	Transverse Bending In-plane Extension In-plane Shear	
Doubly Curved Shell	Transverse Bending In-plane Extension In-plane Shear	
Acoustic Cavity	3D Acoustic Cavity	

SEA model with junctions can be seen in Figure 3.5 colored with red. Point junctions transfer the vibrational energy between two or more SEA subsystems which are physically coupled at a point in space. A point junction represents connections between subsystems that are small compared with a wavelength of sound wave. Line junctions connect the subsystems along a straight or curved line segment. It describes structural connections between subsystems that are continual and large compared with a wavelength of sound wave. Area junctions transmit the energy between cavities or surrounding plates or shells that share a common bounding area or face. VA One features a sophisticated mechanism for determining junctions and calculates the coupling loss factors automatically.

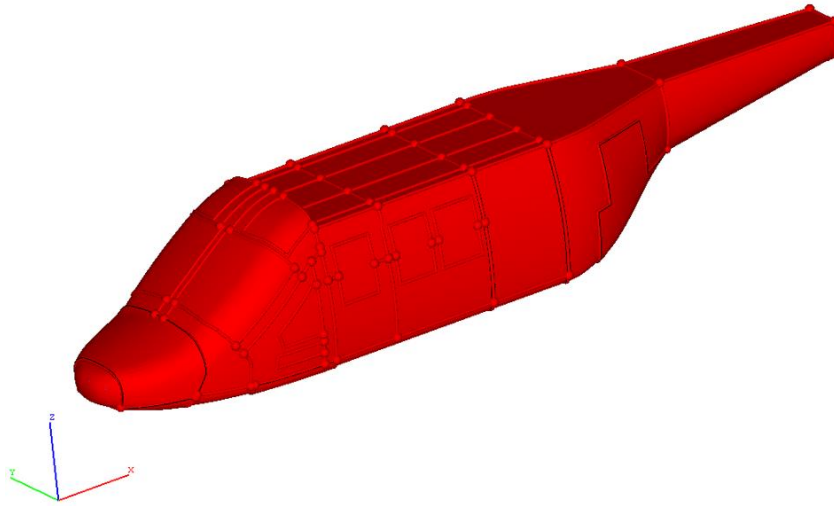


Figure 3.5 SEA model with junctions

In aircraft structures and also in TLUH, the major structure type is the ribbed panel. Generally, beams are used to influence the vibrational behavior of panel by increasing stiffness and inertia. The weight of the panel and its damping usually increases by about 50% and by a factor 2, respectively. The resonant frequencies are found by including the effects of the ribs. Consequently, modal density of structure is affected. Ribbing also causes the sound insulation and increases the radiation resistance. A reduction in radiated power from ribbed panel is approximately 10 times less compared to the simple panel. As a result of these factors, a reduction in panel displacement and acoustic responses are achieved [39]. At low frequencies, ribbed panel behaves as a stiffer orthotropic panel. However, at high frequencies the ribs and the panel behave independently [40].

In VA One, a modal formulation is used to compute the vibro-acoustic properties of a ribbed plate. The formulation used for a ribbed panel is based on thin shell theory. When the bending wavelength in the base plate or shell is smaller than the rib spacing, the rib dynamics are included by smearing the rib's mass and stiffness into the base panel properties. Otherwise, the rib dynamics are included as rigid boundaries between identical sub-panels with base plate or shell properties.

There should be some property identification for ribbed plates, which can be seen in Table 3.4. Each set of ribs is defined by a uniform spacing, beam physical properties and a ribs section offset from the panel. A space averaged value of the properties is calculated for each set of ribs since the beams have different material and sectional properties.

Table 3.4 Required ribbed plate description

Properties	Description
Area	Cross sectional area of beam
Perimeter	Peripheral length around the section
I_{XX}	Second moment of area of the section about the beam's X neutral axis
I_{YY}	Second moment of area of the section about the beam's Y neutral axis
J_{ZZ}	Polar second moment of area of the section about the beam's shear center
Q_{ZZ}	Torsion constant
D_X	X location of the shear center relative to the neutral axis of the section
D_Y	Y location of the shear center relative to the neutral axis of the section
Spacing Mean	Mean value of the spacing between the ribs
Centroid Offset	Offset of the rib centroid from the neutral axis of the underlying skin panel

The structure of forward fuselage extends from front of the fuselage to the end of the cockpit. Front fuselage is composed of 31 structural subsystems. Front fuselage SEA subsystems are presented in Figure 3.6 and Table 3.5 in detail.

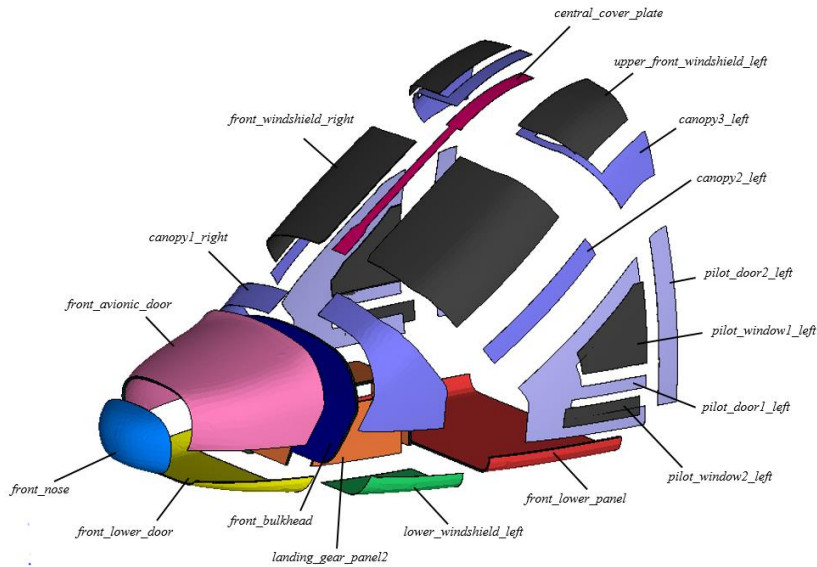


Figure 3.6 Front fuselage SEA subsystems

Table 3.5 Front fuselage SEA subsystems identification

Subsystem Name	SEA Subsystem	Material/ Structure
front nose	Doubly curved shell	Composite
front avionic door	Singly curved shell	Composite
front lower door	Singly curved shell	Composite
canopy1-3	Singly curved shell	Composite
pilot door1-2 left & right	Singly curved shell	Composite
lower windshield left & right	Singly curved shell	Opticor
front windshied left & right	Singly curved shell	Polycarbonate
upper front windshield left & right	Singly curved shell	Polycarbonate
pilot window1-2 left & right	Singly curved shell	Opticor
landing gear panell1-5	Flat plate	Sandwich panel
front bulkhead	Flat plate	Sandwich panel
front lower panel	Flat plate	Skin-Longerons-Frames
central cover plate	Singly curved shell	Metallic shell

Average beam properties in both direction for “front lower panel” to build a model as a ribbed plate is provided in Table 3.6 below.

Table 3.6 Beam properties of “front lower panel”

Parameter	Frame (I Beam)	Unit
Area	506	mm ²
Perimeter	592	mm
I _{xx}	2934105	mm ⁴
I _{yy}	35736	mm ⁴
J _{zz}	2969841	mm ⁴
Q _{zz}	518	mm ⁴
Centroid-Panel Center Distance	101	mm
Centroid-Shear Panel Distance	0	mm
Spacing	419 & 550	mm

Center fuselage is the zone between cockpit end and the frame behind the fuel tank. Upper limit for the center fuselage is cabin upper deck. Mid fuselage is composed of 62 SEA subsystems.

Mid fuselage SEA subsystems are presented in Figure 3.7 and in Table 3.7 in detail. Average beam properties for lateral beams and longitudinal longerons are also provided through Table 3.8.

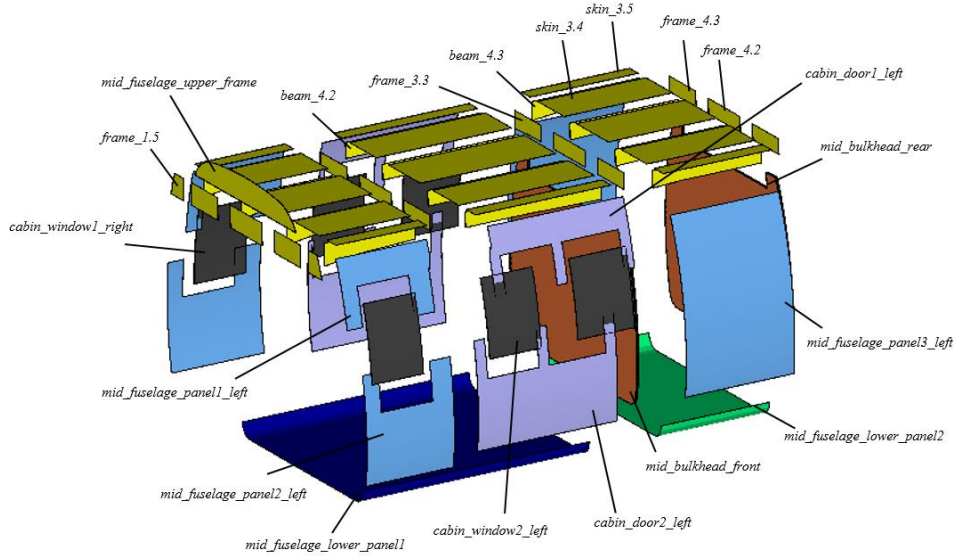


Figure 3.7 Mid fuselage SEA subsystems

Table 3.7 Mid fuselage SEA systems identification

Subsystem Name	SEA Subsystem	Material/ Structure
cabin window1-3 left & right	Singly Curved Shell	Opticor
mid fuselage panel1-3 left & right	Singly Curved Shell	Metallic Shell
cabin door1-2 left & right	Singly Curved Shell	Composite
frame(s)	Flat Plate	Metallic Plate
beam(s)	Flat Plate	Metallic Plate
skin(s)	Flat Plate	Metallic Plate
mid fuselage upper frame	Flat Plate	Metallic Plate
mid fuselage lower panel 1-2	Flat Plate	Skin-Longerons-Frames
mid bulkhead front	Flat Plate	Sandwich
mid bulkhead rear	Flat Plate	Sandwich

Table 3.8 Beam properties of “mid fuselage lower panel1-2”

Parameter	Longeron (I Beam)	Frame (I Beam)	Unit
Area	499	515	mm ²
Perimeter	583	599	mm
I _{xx}	2859046	3019052	mm ⁴
I _{yy}	31674	40742	mm ⁴
J _{zz}	2890720	3059794	mm ⁴
Q _{zz}	516	538	mm ⁴
Centroid-Panel Center Distance	101	101	mm
Centroid-Shear Panel Center Distance	0	0	mm
Spacing	740	700	mm

For “mid fuselage lower panel2” only longeron beam properties of “mid fuselage upper panel1” are used except spacing values. The spacing value is 1050 for this subsystem.

In the center fuselage subsystems, the components around the cabin cavity together with the whole upper deck region as shown in Figure 3.8 are treated and insulated acoustically. A type of soft lining manufactured by TI&A S.p.a. will be used to reduce to level of noise. The thickness and related absorption coefficient provided by the company can be seen in Table 3.9.

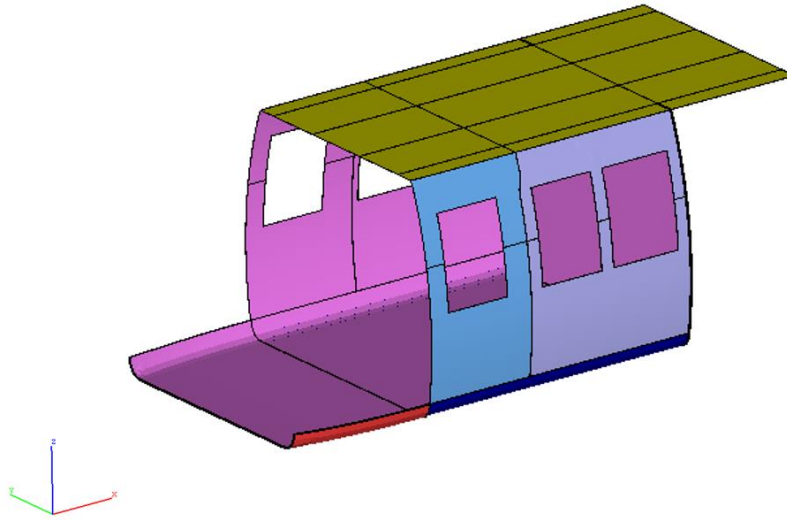


Figure 3.8 Acoustically treated components

Table 3.9 Absorption coefficient for Flexed Foam

ACOUSTICAL ABSORPTION COEFFICIENTS FOR FLEXED FOAM(metric sabins/m ²)							
ASTM C 423 and E 795, Type A Mounting							
	Octave Band Center Frequency (Hz)						
Thickness	125	250	500	1000	2000	4000	NRC
25 mm (1 inch)	0.15	0.30	0.71	0.94	0.97	0.79	0.75

Rear fuselage stands between the fuel tank and the tail cone. There are 4 SEA subsystems, as shown in Figure 3.9.

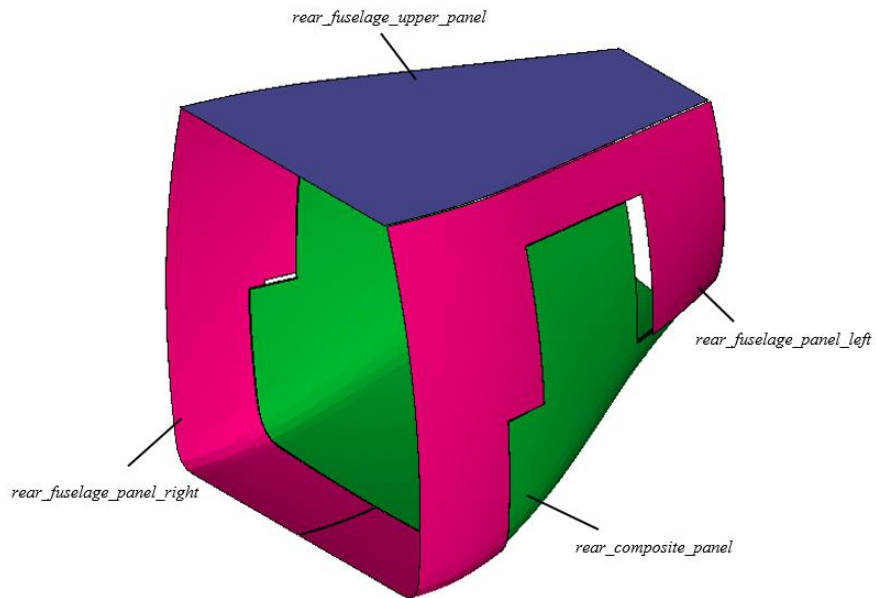


Figure 3.9 Rear fuselage SEA subsystems

Table 3.10 Rear fuselage SEA systems identification

Subsystem Name	SEA Subsystem	Material/ Structure
rear fuselage upper panel	Flat Plate	Skin-Longerons-Frames
rear fuselage panel left & right	Singly Curved Shell	Skin-Longerons-Frames
rear fuselage composite panel	Doubly Curved Shell	Composite

The beam properties for the “rear fuselage upper panel” and “rear fuselage panel left & right” are presented in Table 3.11.

Table 3.11 Beam properties of “rear fuselage upper panel”

Parameter	Longeron (L Beam)	Frame (C Beam)	Unit
Area	412	133	mm ²
Perimeter	583	329	mm
I _{xx}	912570	250635	mm ⁴
I _{yy}	891373	3750	mm ⁴
J _{zz}	180651	254444	mm ⁴
Q _{zz}	277	29	mm ⁴
Centroid-Panel Center Distance	62	37	mm
Centroid- Shear Panel Center Distance	-37	8	mm
Spacing	770	700	mm

Tail fuselage consists of 4 SEA subsystems, as shown in Figure 3.10.

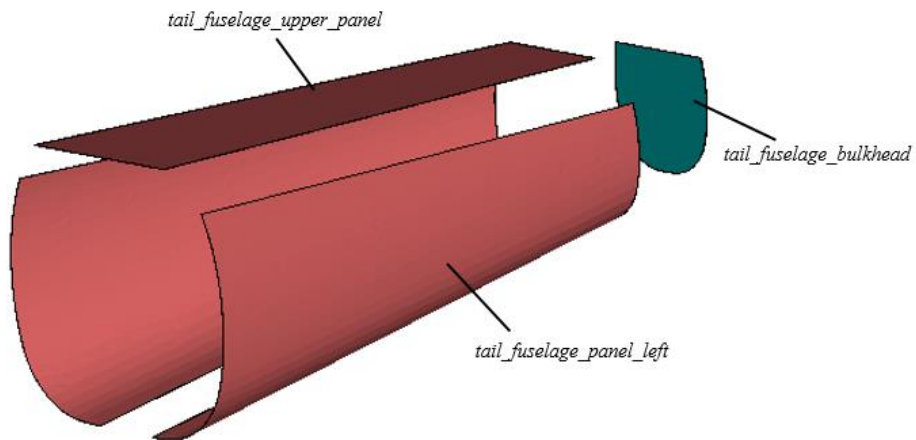


Figure 3.10 Tail fuselage SEA subsystems

Table 3.12 Tail fuselage SEA systems identification

Subsystem Name	SEA Subsystem	Material/ Structure
tail fuselage upper panel	Flat Plate	Skin-Longerons-Frames
tail fuselage panel left & right	Singly Curved Shell	Skin-Longerons-Frames
tail fuselage bulkhead	Flat Plate	Metallic Plate

Table 3.13 Beam properties of “tail fuselage upper panel”

Parameter	Longeron (C Beam)	Frame (L Beam)	Unit
Area	80	233	mm ²
Perimeter	196	209	mm
I _{xx}	52305	60737	mm ⁴
I _{yy}	1189	65833	mm ⁴
J _{zz}	53494	126571	mm ⁴
Q _{zz}	18	406	mm ⁴
Centroid-Panel Center Distance	37	26	mm
Centroid- Shear Panel Center Distance	-4	-13	mm
Spacing	410	500	mm

The volumes inside the helicopter are divided into 13 SEA acoustic subsystems. SEA acoustic cavities are volume-modeling subsystems used to predict sound pressure levels. “front cavity”, “cabin cavity”, “tail cavity”, “rear cavity” and spaces between the frames and longerons of upper deck are identified as air. Internal SEA acoustic cavities are presented in Figure 3.11.

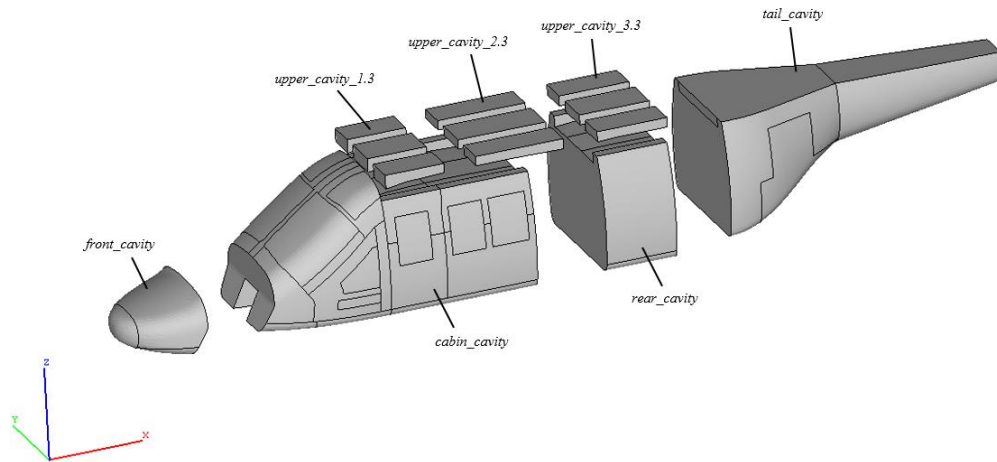


Figure 3.11 Internal SEA cavities

The volumes outside the helicopter are divided into 71 SEA subsystems can be seen in Figure 3.12. These cavities surround the upper panels of the helicopter to simulate fluid (air)- outside the helicopter. Sources inject energy into external cavities, this energy propagates along the various transmission paths into vibro-acoustic system and arrives at a cabin cavity which is location of interest.

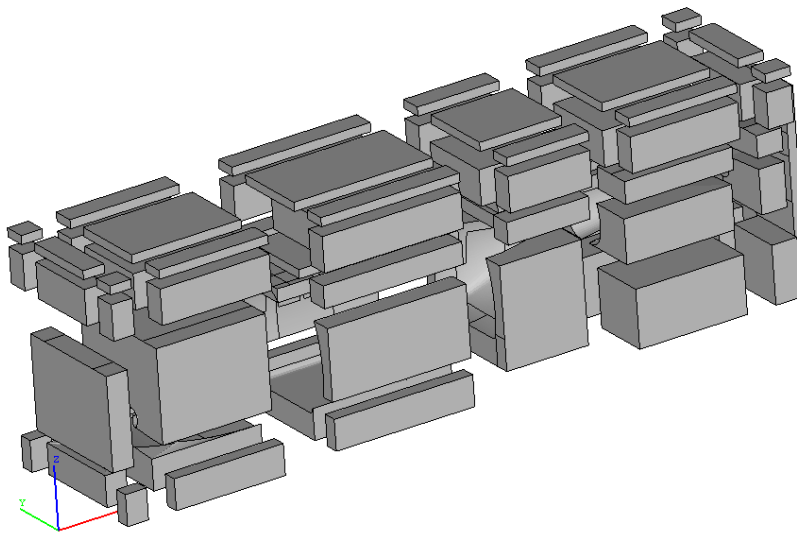


Figure 3.12 External SEA cavities

3.3.1.1 Dynamic Properties and Loss Factors of SEA Subsystems

All the input parameters such as modal densities, damping loss factors, and coupling loss factors were evaluated and identified for the analysis. These parameters are critical to determine the energies of the modal groups and also for transfer paths. The preferred frequency range is from 125 Hz to 20000 Hz for this analysis, which is important for consumer's conformity and also requirements for laws and regulations.

It is also required to define damping loss factors for each subsystem beside the material properties. Damping loss factor is a parameter that determines the amount of sound energy loss through a material. It was defined 0.02 for all panels, 0.01 for all external cavities. The damping loss factor of the cabin cavity and other internal cavities was computed according to all treatments applied to the faces connected to panels. It is taken default 0.01 if there does not exist any acoustical treatment.

Coupling loss factors are automatically evaluated after the junction definition by using VA One. It was correctly assigned for each junction coincident with the geometrical boundaries of the structural parts. The software uses wave approach to evaluate the coupling loss factors between the subsystems.

Modal density in a certain band of frequencies is defined as the number of modes in band divided by the width of that band in radians per second. Therefore, its unit is number of modes per radian/sec. It is used to calculate the number of modes available to receive and store energy in a subsystem. In SEA analysis, energy is settled dominantly in resonant modes. The sum of all modal energies is the overall energy for each subsystem. Therefore, the number of resonant frequencies per frequency band become important. The subsystems of the helicopter were created in the manner that they have modes as many as possible. The higher modal density provides the greater storing energy capacity. The SEA method is applicable when the number of modes of the subsystems is high enough. Practically, in any SEA application, the minimum mode number of a subsystem for the applicability of SEA is set as 3 modes per band [41]. However, in some studies, this value is set to 5 or 10 modes per band and the results are experimentally verified [42].

It is found that the most subsystems are suited for SEA modelling above 125 Hz when the number of natural modes and modal density of the front and mid fuselage of the simulated SEA model are examined. However, components considered in sound energy flow path with low modal density up to 1000 Hz are canopy in forward fuselage, upper deck of the helicopter in center fuselage and bulkhead of the tail cone. This is not surprising as the structure of forward fuselage should be stiffer due to bird strike concerns. Additionally, beams and frames in the upper deck region as shown in Figure 3.15 form the stiff primary support structure of the helicopter. The number of modes of these subsystems up to 1000 Hz can be seen in Figure 3.13 and Figure 3.14.

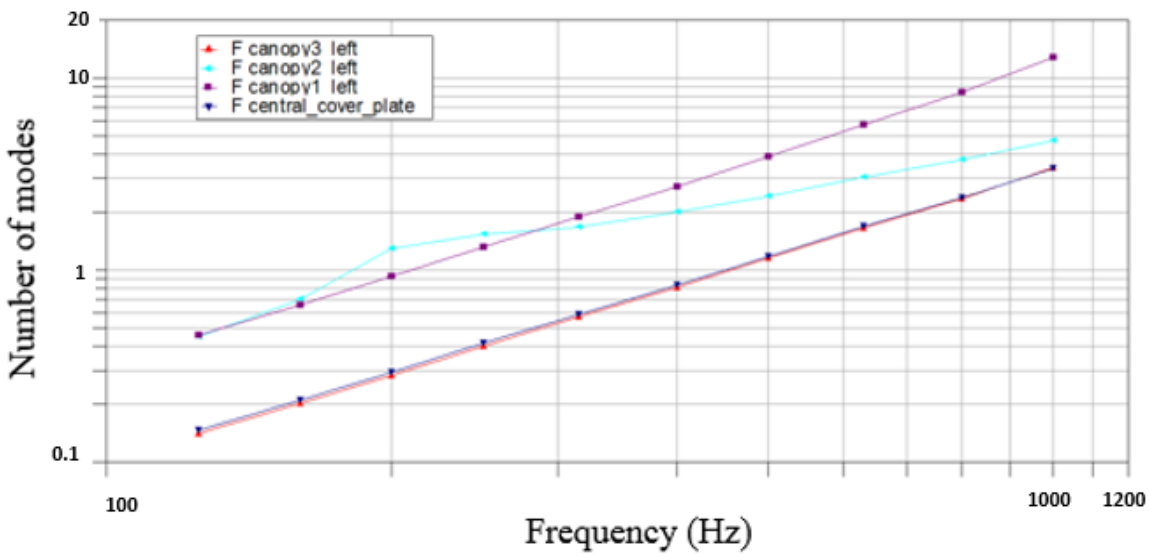


Figure 3.13 Mode count for front fuselage SEA subsystems

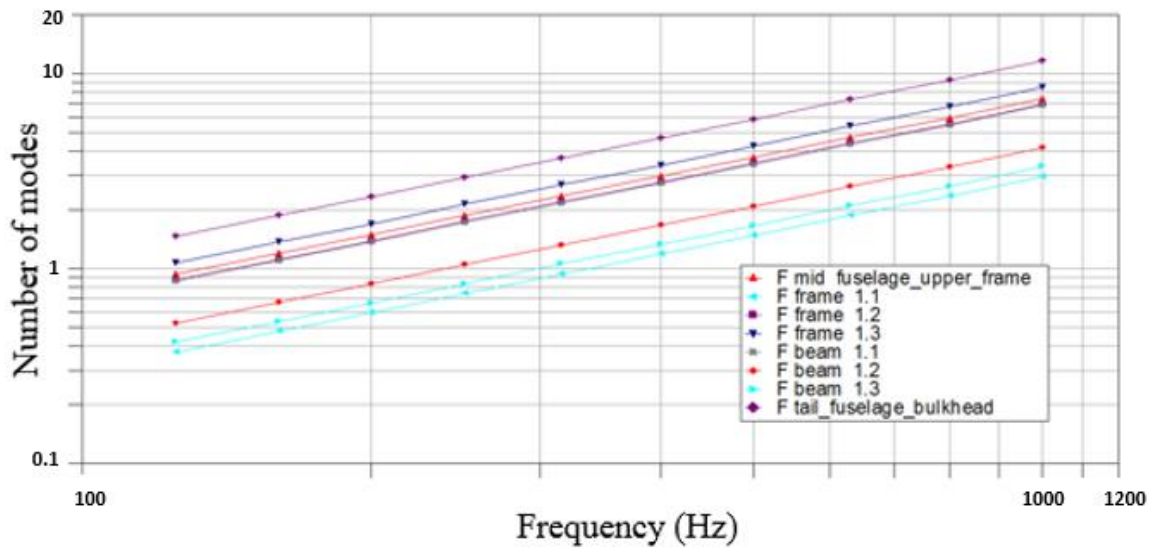


Figure 3.14 Mode count for mid fuselage SEA subsystems

When the number of modes of subsystems are examined, it is observed that, especially at low frequencies, some of the subsystems have modes under value one which is irrational. The reason of that SEA method could not locate any mode, therefore some of subsystems do not store energy at that frequency bands. This affects the other properties of the structure like radiation efficiency, and response of the structure and hence the vibration levels. Additionally, up to 1000 Hz, the mentioned subsystems have modes under value 10 which is critical mode count for SEA validity.

During the modal evaluation of the SEA subsystems, some subsystems of the helicopter SEA model shows low modal density due to high stiffness, e.g. “front nose” and “rear composite panel”. When considered the noise sources and the noise paths on the helicopter, it was interpreted that they do not affect the result of the analysis. It should be noted that the mid fuselage is the most important region for the helicopter since the panels that are on the propagating path to the cabin cavity mostly are in this zone. There are also many noise sources around the mid fuselage area.

3.3.2 Hybrid Model

In the second model, subsystems with very few local modes are represented using Finite Element modeling of subsystems. It is important to use sufficient number of elements to describe the expected response of an FE subsystem in a frequency range of interest. The components mentioned in the first part of the section are meshed with triangles shell elements and totaling 69429 in number. An overall view of the Hybrid FE-SEA model of the helicopter can be seen in Figure 3.15. Hybrid junctions are created to calculate the vibration energy transmission between structural or acoustic SEA subsystems and structural or acoustic FE subsystems physically connected. The hybrid junctions appear as blue in the 3D view in Figure 3.16.

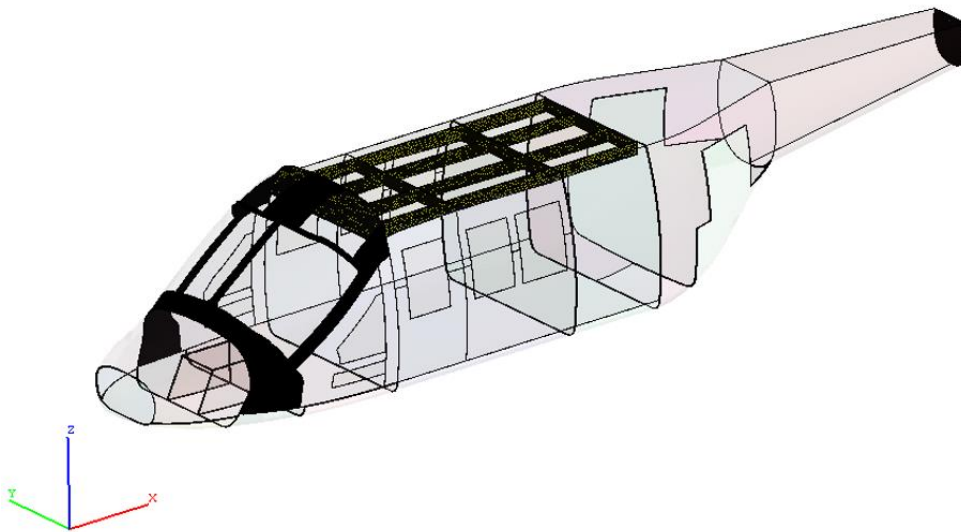


Figure 3.15 Overall view of the hybrid FE-SEA model of the helicopter

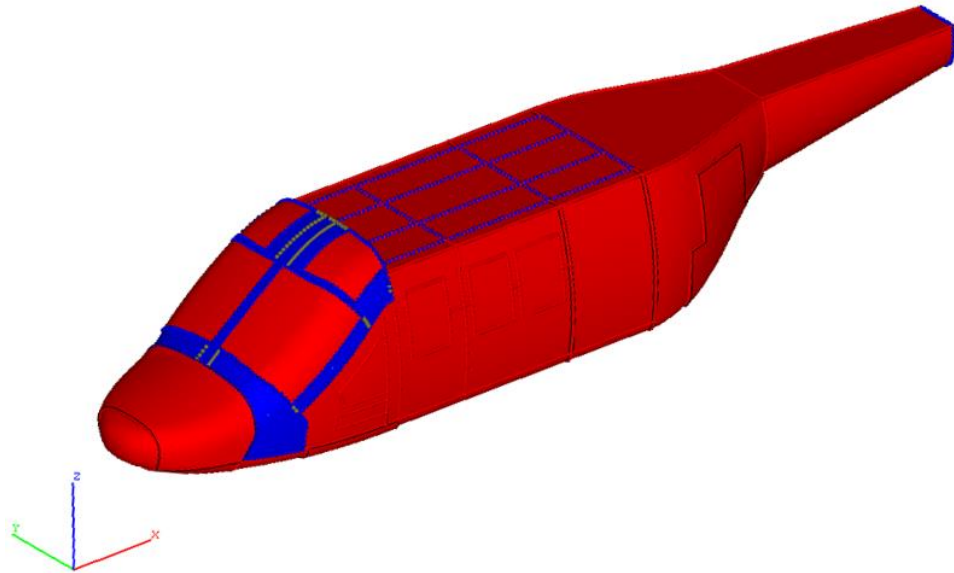


Figure 3.16 Junctions of hybrid FE-SEA Model

The material and physical properties of the meshed subsystems are the same as the ones in the SEA model. Damping loss factors are also assigned to the FE subsystems during the modeling process. Global and local data and related natural frequencies are calculated to generate mass and stiffness matrices for the FE subsystems. The number of modes of the subsystems after modelling with finite elements can be seen in Figure 3.17 and Figure 3.18. The coupled hybrid model is used to describe the response in the frequency range 125 Hz to 1000 Hz.

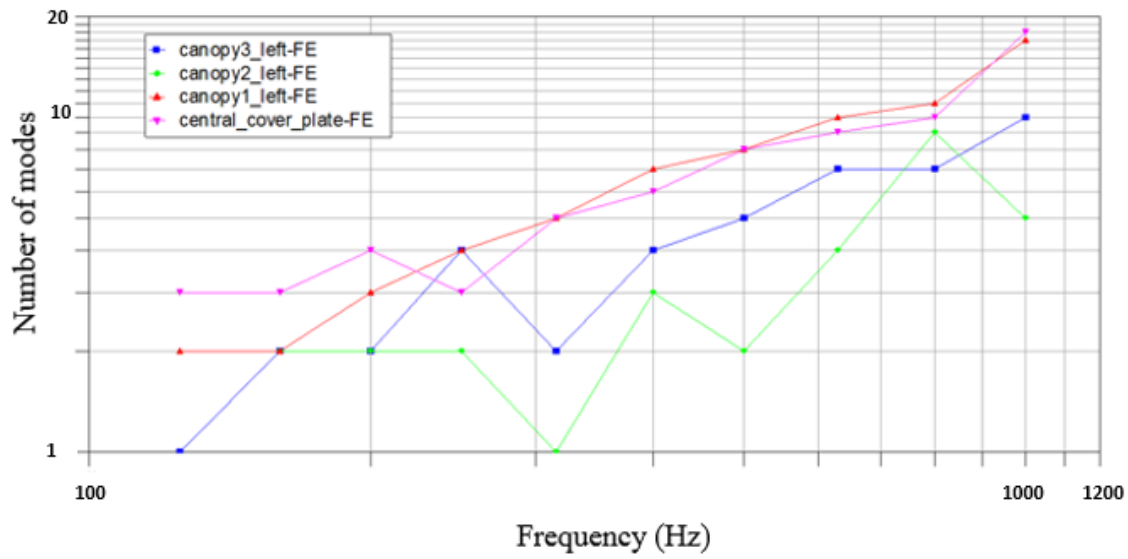


Figure 3.17 Internal acoustic cavities modal densities

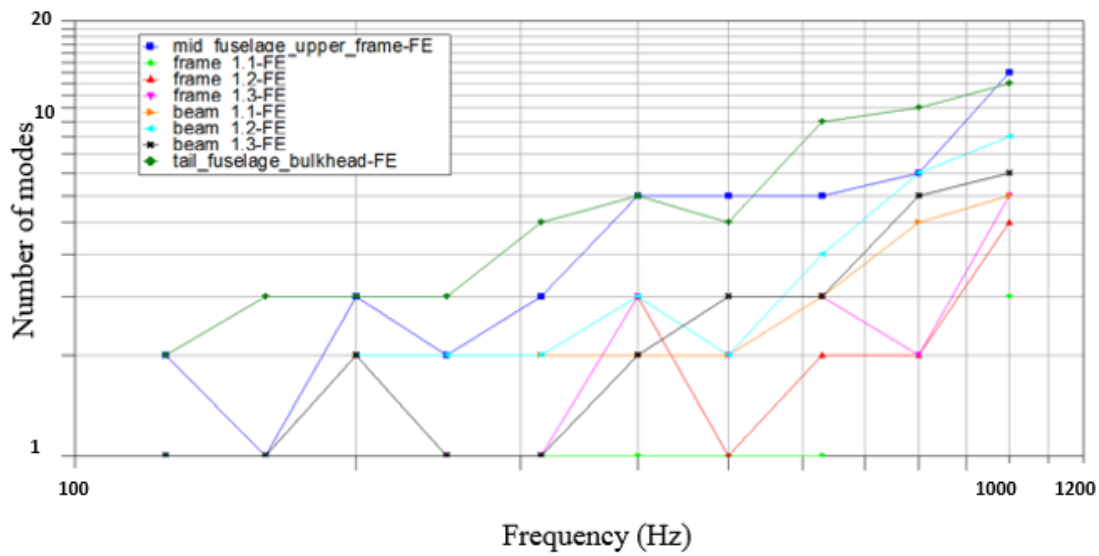


Figure 3.18 Internal acoustic cavities modal densities

After modelling the mentioned subsystems with FE, it is obviously seen that FE method can locate more modes than SEA method. To cover the entire frequency range of interest, the analysis must take into account the large number of acoustic and structural modes contributing to the dynamic response. Finite Element formulation enables more efficient analysis of systems in which a limited number of modes are being excited. In the second hybrid model, some structures are modelled with SEA method which is applicable according to critical mode count and the others are modelled with FE method. SEA tends to work best for higher modes where there are many natural frequencies close together. This is opposite of Finite Elements which work best for lower modes.

SEA and hybrid models are constructed and applicability of the models is checked for related frequency ranges. Estimation of power inputs and the results are presented in Chapter 4 in octave bands.

CHAPTER 4

ANALYSIS AND RESULTS

4.1 Power Inputs

In the preliminary design phase of a new product, one of the challenging part of the modelling is to find power inputs since no measurements during any flight can be made. For rotorcrafts, there exists many input excitations contributing the global noise field. Accordingly, the approach for this thesis is to estimate the dominant noise sources in the case of the loudest flight condition. Some is provided from detailed aero acoustic analysis of the helicopter, the other is taken into account based on results of different research works in the literature.

In this analysis, high speed forward flight condition with high operating engine is considered in the model. The flight profile is shown in Table 4.1.

Table 4.1 Flight condition

Flight Condition	Main Rotor (rpm)	313
	Tail Rotor (rpm)	1497
	Speed (KEAS)	150
	Altitude (ft.)	0-15000
	Power (hp)	1255

The main and tail rotor sound levels, engine airborne noise, MGB airborne noise and TBL excitation are implemented to the model. Apart from these, it should be noted that there could not be found any structure borne dynamic load sets since any vibration data has not been monitored yet. If there exists, they should be exerted to the upper deck of the helicopter on which engine mounts and MGB strut lugs stand. As a result, all airborne noise inputs are applied to the exterior acoustic subsystems in terms of constrained pressure as shown in Figure 4.1.

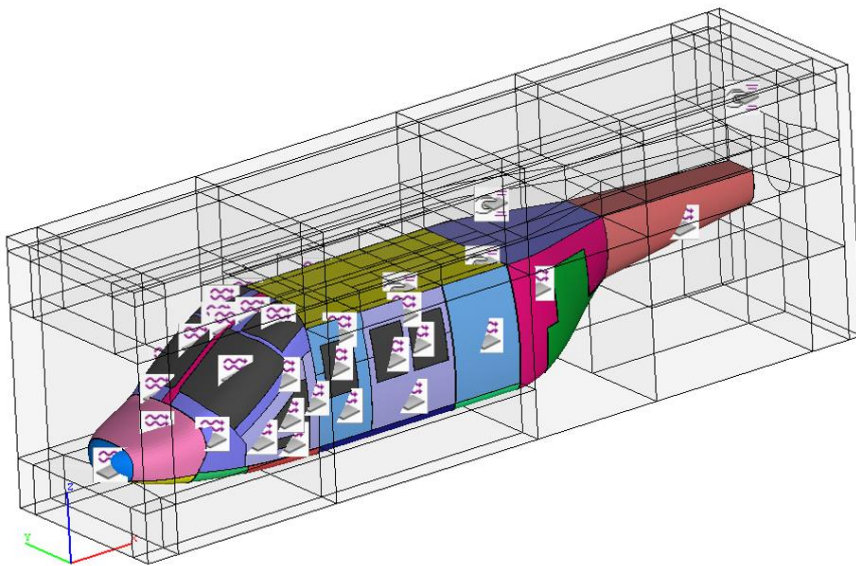


Figure 4.1 External excitations

4.1.1 Main and Tail Rotor Noise

Rotors are the governing aeroacoustic source of helicopters. During the flight, main and tail rotors dominate absolute noise levels especially at low frequency range of spectrum. Rotor and blade design are important parameters for acoustic characteristic. The aerodynamic sound is generated by the operation of rotors at the blade passage frequency and their harmonics.

Methodology and rotor noises are provided from detailed aero acoustic analysis of TLUH. With the ease of computational numerical methods and tools, noise prediction of rotor noise capabilities can be computed.

The propagation of noise can be formulated with integral formulation by exploiting near aerodynamic field around the source. Kirchhoff and Ffowcs-Williams-Hawkings are the common integral methods. Accurate noise values can be predicted by using Kirchhoff integration method while FW-H integral method gives surface pressure fluctuations in terms of integral. Rotor rotational noises are represented with the first and second terms in the FW-H equation.

Aeroacoustic analyses within the scope of TLUH project are planned to be conducted with “PSU-WOPWOP” and “CHARM” programs. Using parameters of rotor, blade geometry, desired flight and environmental condition, load distributions over the rotor blades are generated. Then, an acoustic analysis for near field is conducted with PSU-WOPWOP, a commercial comprehensive noise estimation algorithm. With the final step, standard FFT algorithm post-processes the pressure data in order to determine aerodynamically generated noise components and related frequency spectrum as the dominant external noise. Tail and main rotor sound pressure levels can be seen in Figure 4.2.

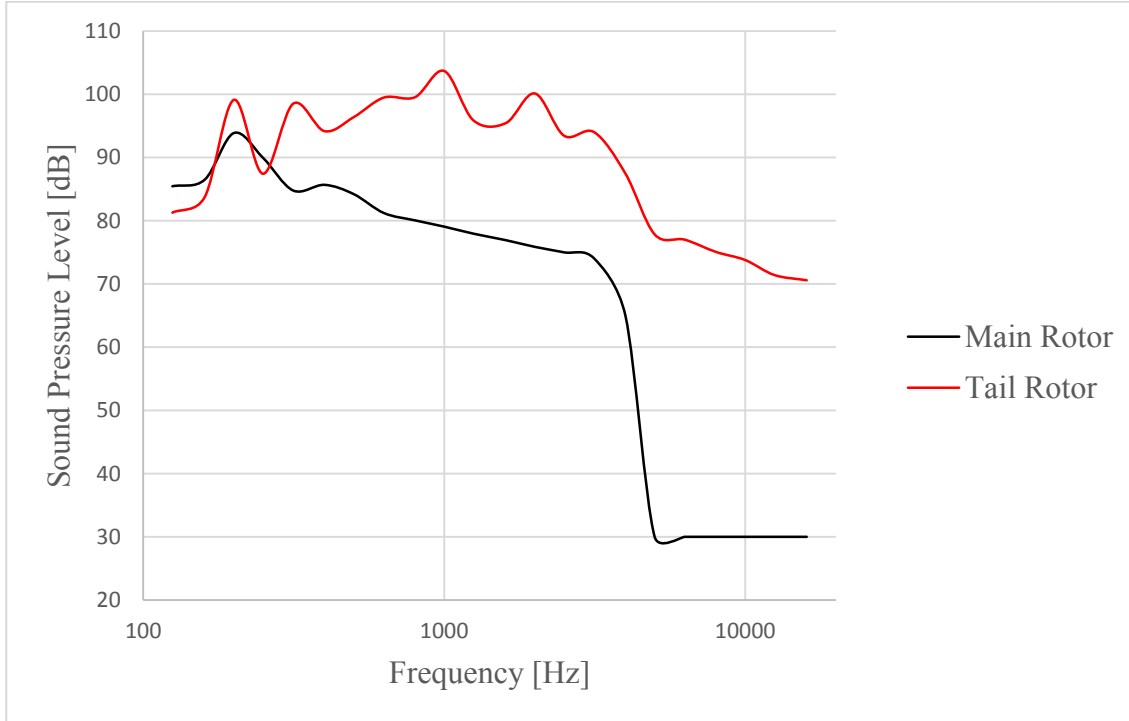


Figure 4.2 Near field pressure levels of main and tail rotors

4.1.2 TBL Noise

The helicopter fuselage skin is excited by high speed airflow during its operations. The unsteady flow over the surface area can be characterized as random pressure fluctuations. These fluctuations can be obtained from measured space-averaged RMS pressure using experimental approach. Besides that, analytical prediction methods have been studied for many years to be formulated based on empirical data. The spectral distribution formula of the pressure field is expressed by Cockburn and Roberson in 1974. They proposed formulae for different pressure environments, attached and separated flow conditions, as shown in Table 4.2. In the expression $\Phi(f)$ denotes the normalized overall mean square fluctuating pressure and f_0 is characteristic frequency.

Table 4.2 Power spectral density formulae for different conditions

Vehicle	Pressure Environments	
Cone Type	Seperated Flow	Attached Flow
Power Spectral Density	$\frac{\Phi(f)U}{q_\infty^2 \delta} = \frac{(P^2 / q_\infty^2)_s}{\left(\frac{f_0 \delta}{U}\right)_s \left\{1 + (f / f_0)^{0.83}\right\}^{2.15}}$	$\frac{\Phi(f)U}{q_\infty^2 \delta} = \frac{(P^2 / q_\infty^2)_A}{\left(\frac{f_0 \delta}{U}\right)_A \left\{1 + (f / f_0)^{0.9}\right\}^{2.0}}$

VA One computes boundary layer flow excitation by using the approach mentioned above with correlation functions. Dynamic pressure loads can be defined in VA One by the parameters listed below [37];

- Nominal flow speed outside of the boundary layer, U_0
- Density of fluid at flight altitude, ρ
- Kinematic viscosity of fluid at flight altitude, ν
- Speed of sound at flight altitude, c_0
- Distance from the leading edge of the TBL to the center of the pressure load on the surface of the subsystem, X_0

Turbulent boundary layer thickness can be computed from the following equations.

$$\delta = 0.37 \frac{X_0}{\text{Re}} \text{ where } \text{Re} = \frac{U_0 X_0}{\nu} .$$

In the analysis, TBL pressure is applied to the SEA subsystems that interact with its outside surroundings displayed in Figure 4.1. All the parameters calculated from related flight condition are defined. Leading edge distance for each subsystem are determined. Fluctuating pressure level is higher in seperated field than attached one. Therefore, seperated boundary layer spectrum is selected while modelling to be conservative.

4.1.3 Main Gear Box Noise

The purpose of the MGB system is to transfer power from the engines to the main rotor shafts, to the tail rotor driveline and to the accessories while providing the required speed reductions or increases. The main gearbox is driven by the engines that are operating at high frequency while the main rotor mast speed is at low frequency. The variation of speed is achieved by the MGB with the gears and reduction ratios.

The power transmission system of TLUH is designed according to international standards. It is composed of the following main systems:

- Main Gearbox (MGB)
- Engine Drive Shafts
- Tail Drive Line
- Intermediate and Tail Gearbox

Mesh frequencies which can be found from the kinematical features of TLUH gears are the frequencies where high sound levels are produced. These discrete tonal noise components affect the noise characteristic of helicopter.

It is needed to know sound level arising from gears to take MGB noise into account for cabin acoustic evaluation. In the literature, there are studies in which series of measurements are performed and reported. There are also complex analytical methods which can be used to calculate acoustical energy radiated from gears. For TLUH program, there are not any measured noise data or calculation available of any operational condition since the program is at development phase. Accordingly, in this study as a primary input MGB sound levels are predicted based on two different academic works in which recordings taken on gear box hatch from two different helicopter can be found.

The first study [43] by I. Laskin, F.K. Orcutt and E.E.Shipley in June 1968 analyzed the gearbox noise of UH-1D helicopter developed by Bell Helicopter Textron. They found a computerized methodology to calculate gearbox sound level and compared the results with empirical data which is used for this thesis. The data was acquired from gearbox

casing on four different UH-1D helicopters in cruise operation. They found the most annoying noise occurs at teeth interaction of two gears when loaded.

In their analysis, each individual mesh frequency is emplaced in the related octave bands. The mesh frequencies which are close to two adjacent octave bands are associated equally with both bands. The effect of discrete peak noise appears in the octave bands where related mesh frequency falls in.

During the measurement, the engine and air speed are 6600 rpm and 75-80 knots, respectively. The average sound pressure level of measured data taken from four helicopters is tabulated for one third octave frequency band in Figure 4.3.

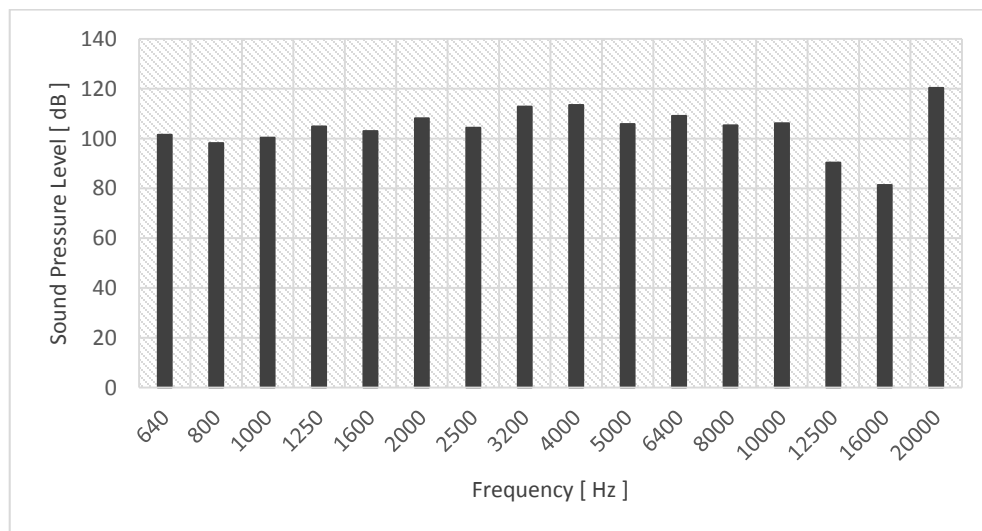


Figure 4.3 UH-1D measured sound pressure levels [43]

The other study [44] carried out by Schomer and Averbuch is a further application of analytical tools used for UH-1D helicopter. In this work, CH-47 power train provided by Boeing-Vertol is investigated. Calculation made by the analytical tools shows good correlation with operational records. Flight measurements are conducted on three different

CH-47 helicopters in cruise condition. The rotor speed is 230 rpm at cruise condition. Average sound pressure level can be seen in Figure 4.4.

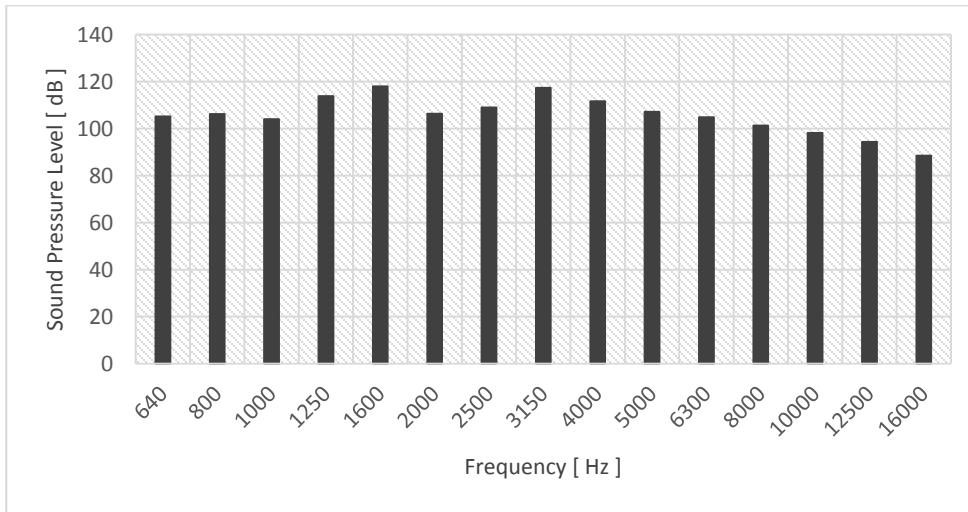


Figure 4.4 CH-47A measured sound pressure levels [44]

When examining the kinematics of the drive systems of mentioned helicopter and TLUH, mesh frequencies almost match with each other. Likewise, power levels are also similar to the Turkish Light Utility Helicopter. As a consequence of these, TLUH gearbox airborne noise levels can be predicted using data of two surveys mentioned above for the analysis.

MGB noise covers dominantly mid to high frequency range. MGB contribution of low frequency bands is assumed 40 dB since low frequency range is confined by the noise associated with the rotors. For high frequency ranges, comparing experimental results of UH-1D and CH-47A, the highest noise level is selected for each octave band to be conservative. In Figure 4.5, estimated main gearbox airborne noise levels are figured for 1/3 octave bands.

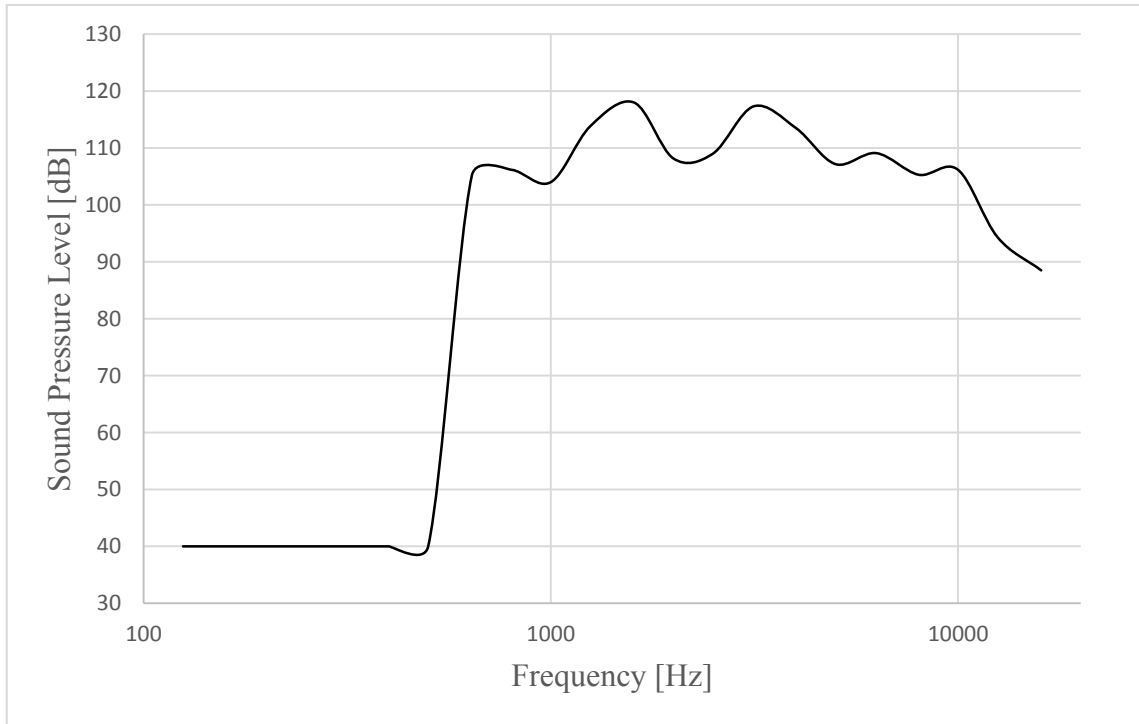


Figure 4.5 MGB airborne noise estimation of TLUH

4.1.4 Engine Noise

The acoustic testing is performed by the manufacturer to examine whether TLUH engine exhaust noise provides acceptable aero-acoustic behavior or not. In this test, measured engine 1/3-octave band sound power levels are obtained at the engine operation with 1285 SHPC. Calculations are done using measurement data with a reference sound source positioned in 4 different locations around the engine. Sound pressure levels, presumably dominated engine exhaust and case noise can be seen in Figure 4.6.

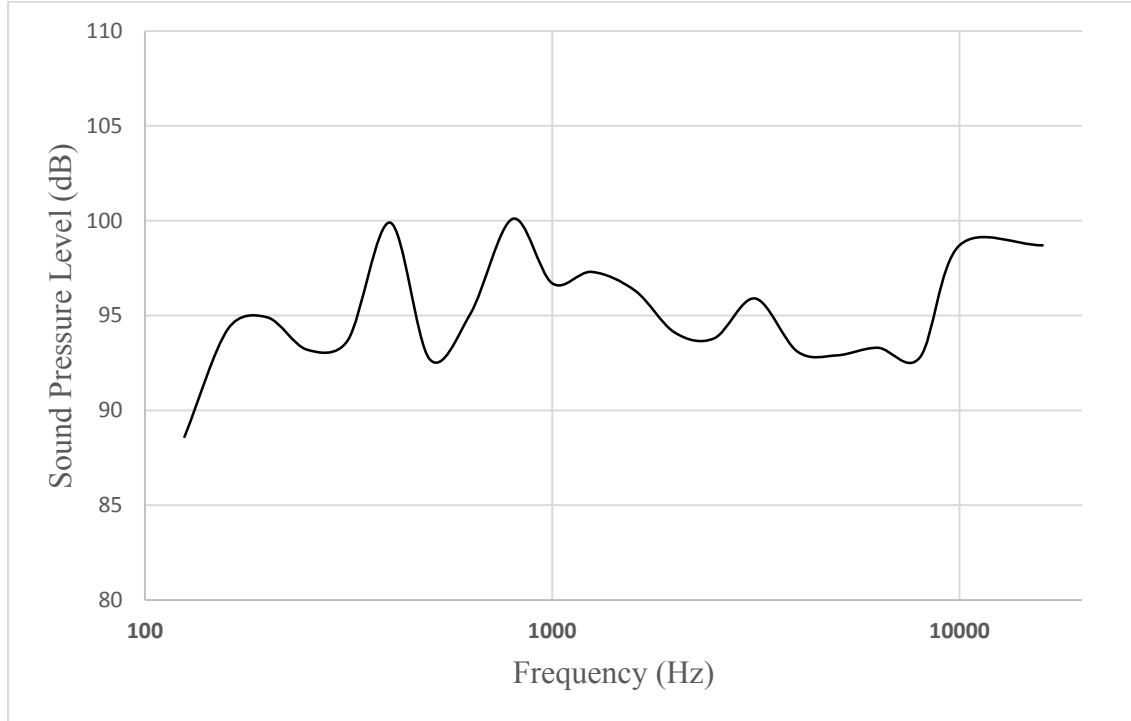


Figure 4.6 Engine exhaust measured pressure levels

4.2 Prediction of Helicopter Cabin Noise Level

The results are obtained for SEA model from 125 Hz to 16000 Hz in 1/3rd octave bands for the defined flight condition. In the second part, hybrid FE-SEA model are solved in the frequency range from 125 Hz to 1000 Hz.

4.2.1 SEA Model Results

As displayed in Figure 5.7, the highest sound level is observed at 125 Hz one-third octave band. The power inputs from the main and tail rotor at low frequencies due to their nominal rotational speeds are the causes of the high pressure levels in the cabin cavity. However, when A-frequency-weighting is applied to the results, mid frequency range becomes dominant sound contributors in the overall sound level. Main gearbox is the

pivotal contributor in mid to high frequency range. The peaks in 1000 Hz to 5000 Hz range due to the gear teeth interactions of the MGB system at mesh frequencies and their harmonics. From 10000 Hz and above, high rotational speed of engine noise dominant. The appearance of the three prominent peaks is attributed to the coincidence of the resonant frequencies of the cabin cavity air and structural elements.

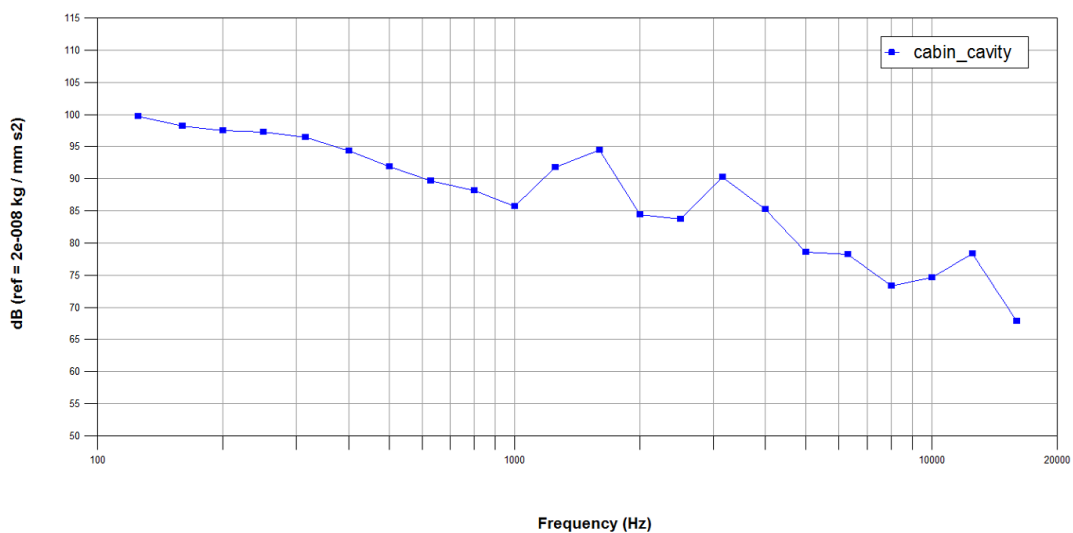


Figure 4.7 SEA estimation of TLUH passenger cabin without NCT

In Figure 4.8, the results are compared with measured cabin noise levels of similar helicopters in 1/1 octave bands. Agusta 109 and Bell 212 are in the same segment with the simulated helicopter. Measurement data during operation for both helicopters are taken from [45]. As can be seen in Figure 5.8, the sound pressure levels display similar behavior.

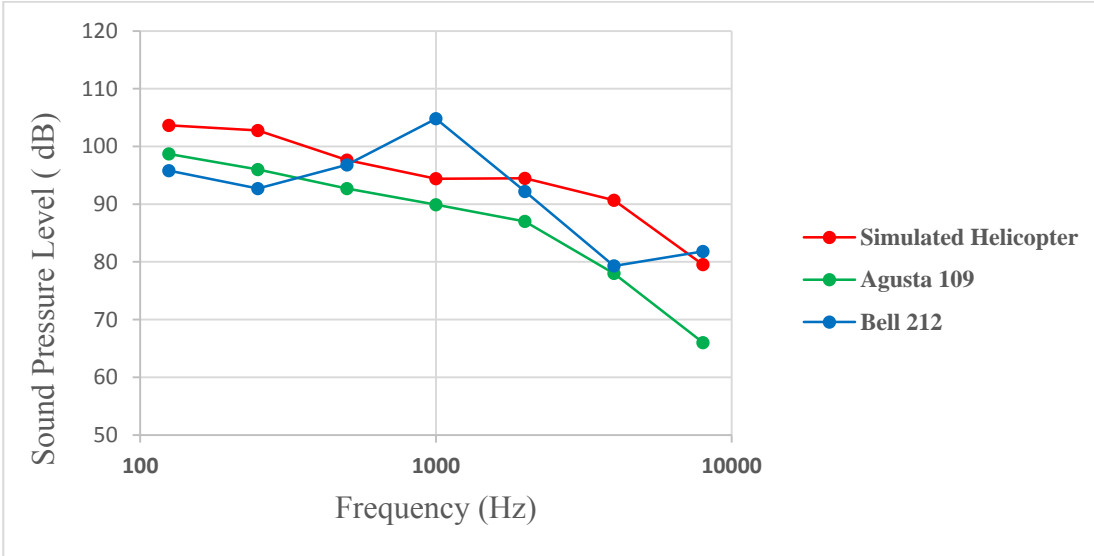


Figure 4.8 Comparison of helicopter cabin noise levels with similar helicopters of comparable power

As mentioned in the section of model development, the structures surrounding the cabin cavity in center fuselage are covered with the very simple insulation material. The average acoustic response in cabin cavity is stated and compared to results with no treatment in Figure 4.9. Looking in detail, although the noise reduction is achieved through all the frequencies, it can be seen the foam is more effective at high frequencies. The noise reduction is nearly 2 dB at low frequencies which turns about 20 dB at high frequencies.

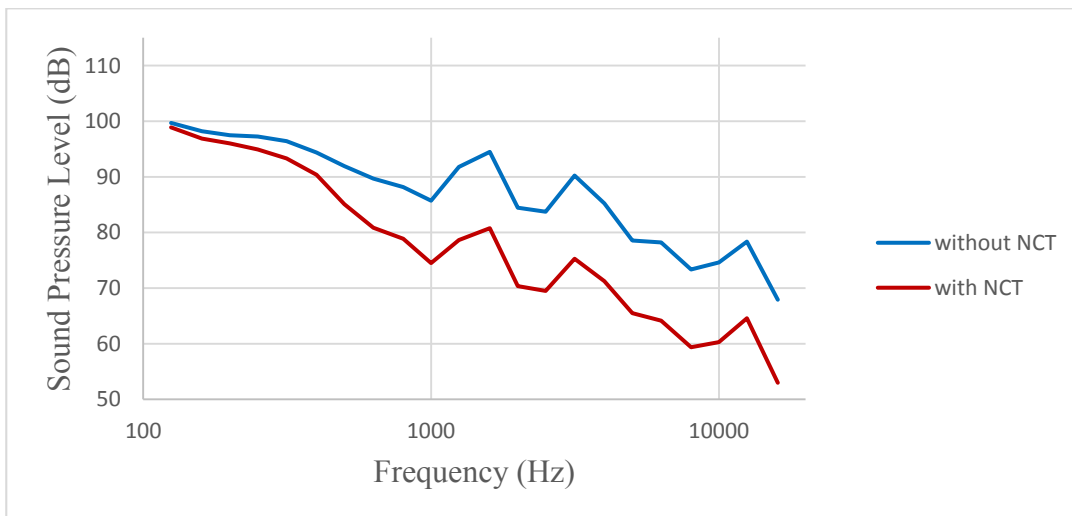


Figure 4.9 Comparison of SEA sound pressure results with and without NCT

4.2.2 FEM-SEA Hybrid Model Results

Canopy, upper deck frames, upper deck beams and tail bulkhead are modelled with FEM in the second model as they have low modal density. The sound pressure levels are indicated in Figure 4.10 from 125 Hz to 1000 Hz in 1/3rd octave bands.

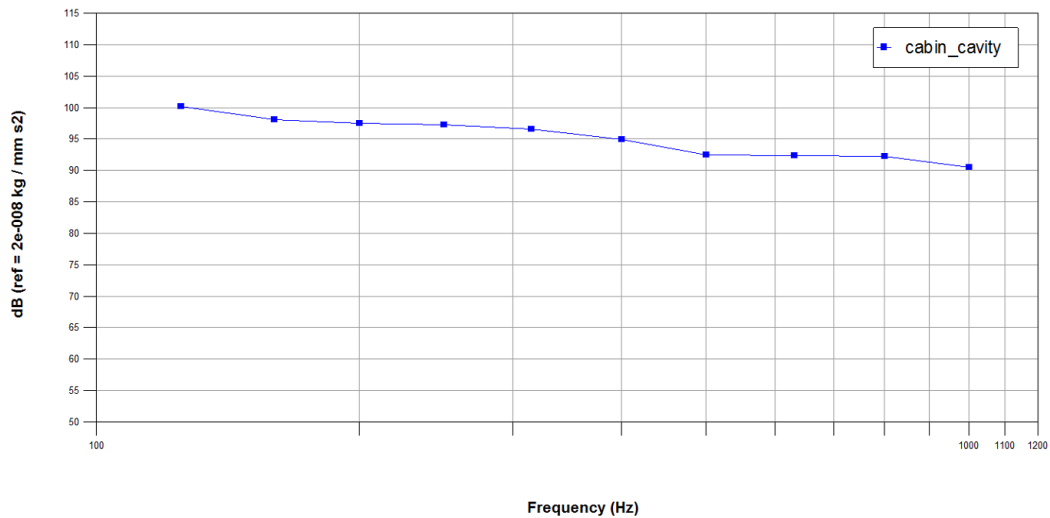


Figure 4.10 Hybrid estimation of TLUH passenger cabin without NCT

In Figure 4.11, comparison between the results of SEA model and hybrid model is shown. These results are obtained from 125 Hz to 1000 Hz in 1/3rd octave band center frequencies. Sound levels increase at all discrete frequencies. However, it is clearly observed that sound level increases starting at 500 Hz band.

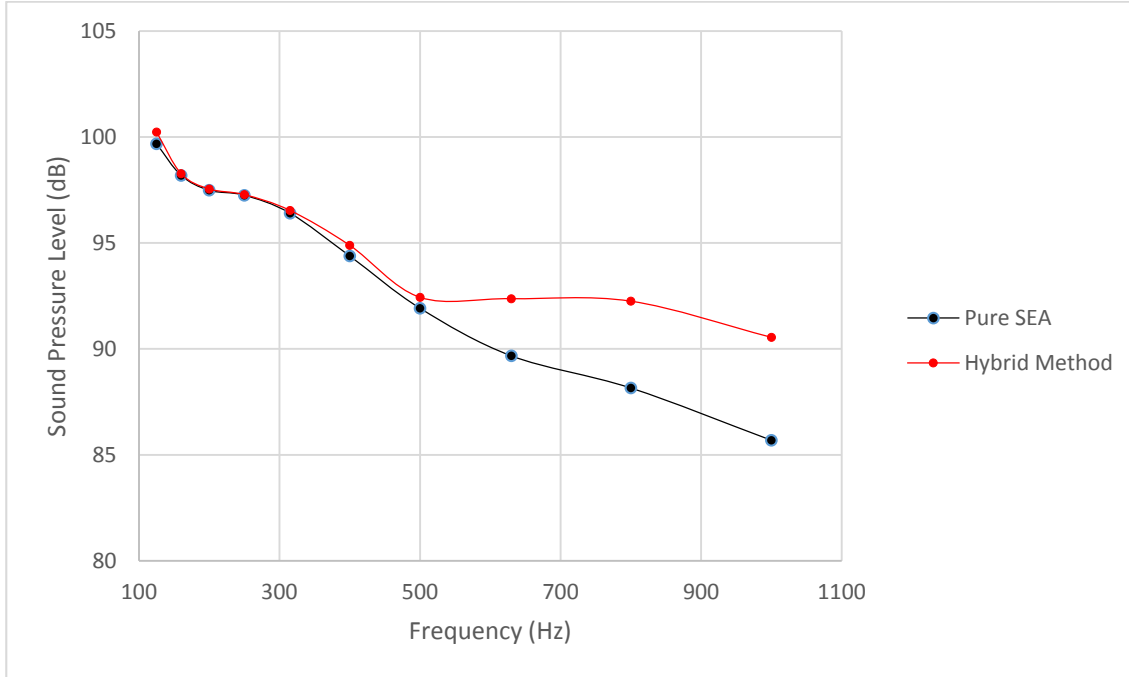


Figure 4.11 Hybrid-SEA comparison

In Figure 4.12, the two lines at the top show sound pressure levels for both models while the two lines below show the total number of resonant frequencies for both models in frequency range, 125 Hz to 1000Hz. As it is seen, the number of resonant frequencies in FE-SEA hybrid model is higher than that in SEA model for all frequencies which is same trend with the sound pressure level difference between SEA and FE-SEA hybrid model. This is expected as the sound energy storage of the FE subsystem is increased by FEM.

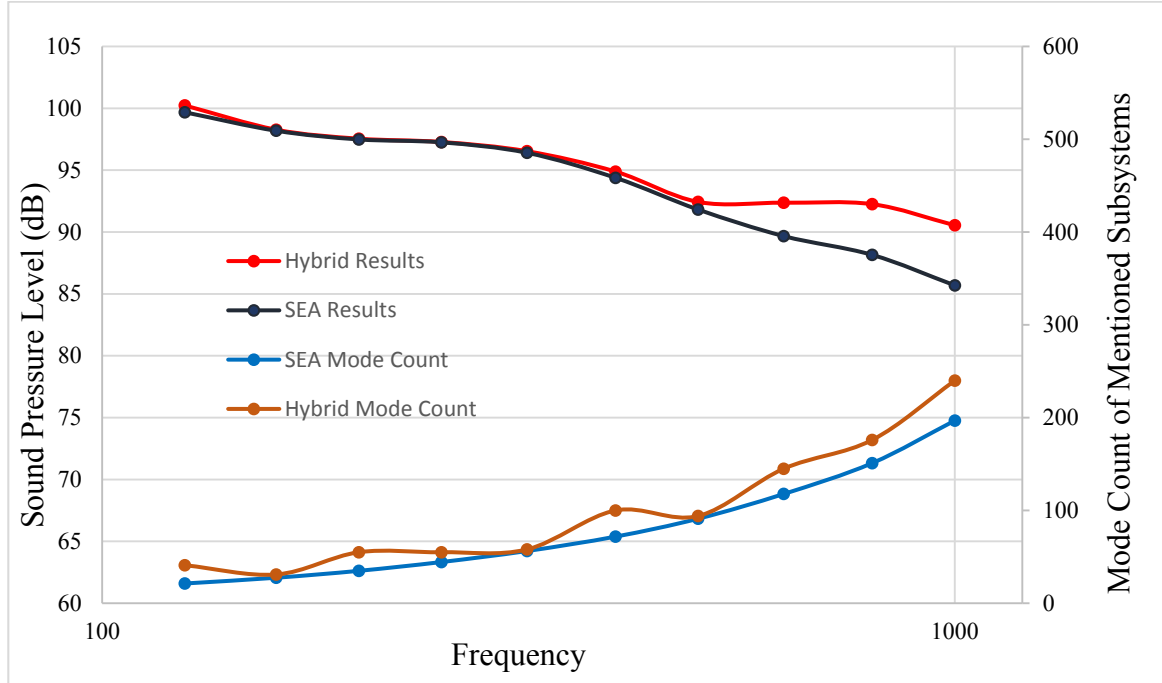


Figure 4.12 Sound Pressure Level- Mode Count comparison

As can be seen from Figure 4.11, pure SEA and hybrid method results are similar at low frequencies as opposed to results at mid frequencies. However, it is expected that inclusion of finite element affects the results more at low frequencies when compared to pure SEA ones. In Chapter 3, it is mentioned that subsystems except canopy in forward fuselage and frames and beams in upper deck region are suited for SEA, even at low frequency, according to modal density procedure. Additionally, it is assumed that canopy structure, frames and beams are located in sound energy flow path. Therefore, they are modelled with FEM in the second hybrid model to get more accurate results.

Figure 4.13 and Figure 4.14 shows energy distribution of the subsystems for SEA and hybrid FE-SEA method, respectively. It shows that the representation of the regions using FEM is not on energy flow paths at low frequency despite the assumption made in Chapter 3. The analysis of the energy flow shows power contributions by side panels and windows are larger than other panels to cabin cavity. The side panels and windows are sensitive

structures in the low frequency range. Sensitive panels transfer the noise from the exterior source to the interior cavity. They are very efficient radiator and bending waves are easily converted into radiated noise through them. This implies that canopy, frames and beams have minor contribution to the global cabin noise at low frequencies even if they are modelled with FEM. FE method provides more modal information compared to SEA method. Yet, it may not enough to change energy flow path.

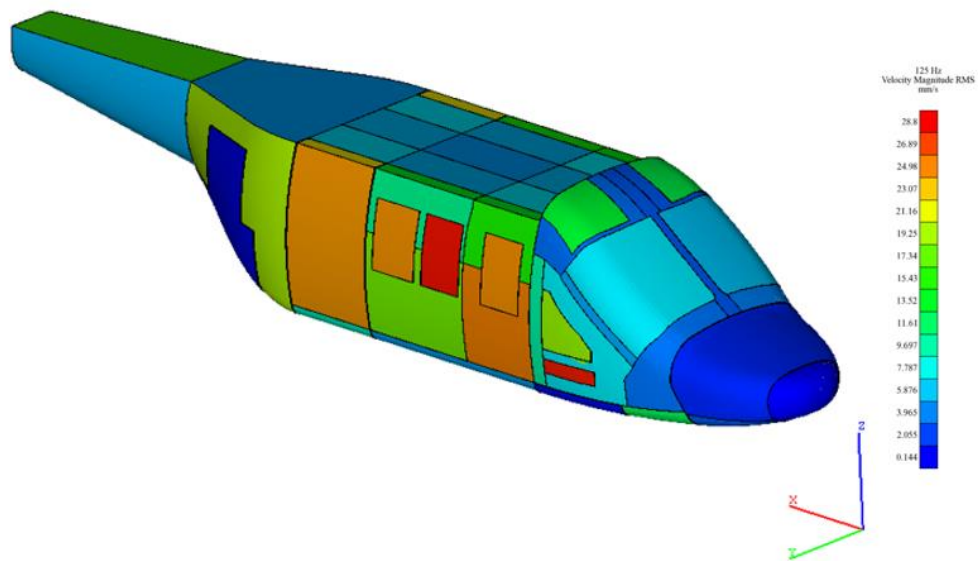


Figure 4.13 Energy flow in SEA model at 250 Hz

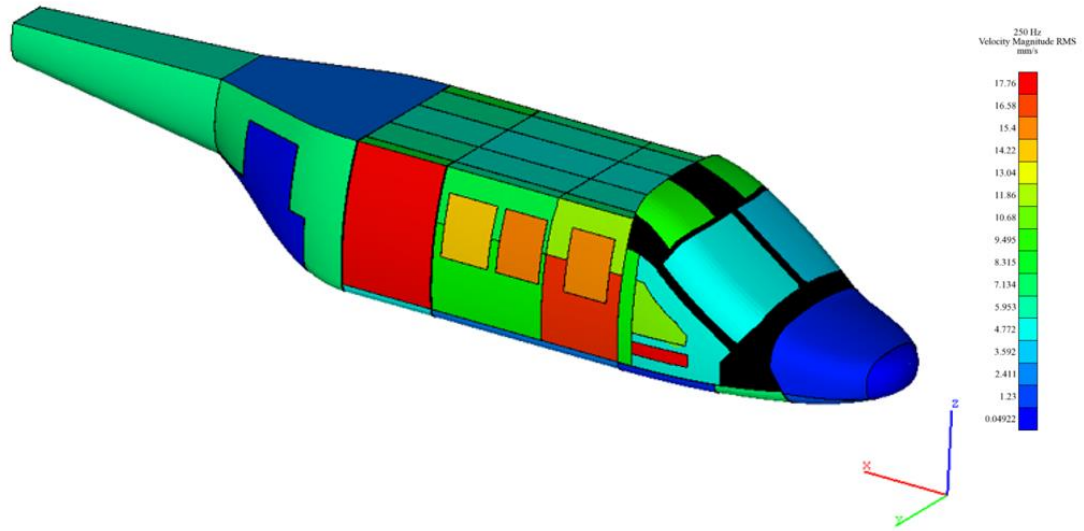


Figure 4.14 Energy flow in hybrid FE-SEA model at 250 Hz

According to results of both analysis, the subsystem with the highest energy level is “mid_fuselage_panel3_left” which is located at side region as mentioned above. If the energy level of this subsystem is compared with subsystems that are parts of canopy structure and upper deck, it is seen that the energy ratio is very small, especially at low frequencies. Figure 4.15 shows the energy level difference between the subsystems. After modelling with FEM, the energy levels of mentioned subsystems are increased. However, the energy ratio is still low despite the increase of energy level after modelling FEM. This also indicates that these structures have little effect on the final results at low frequencies.

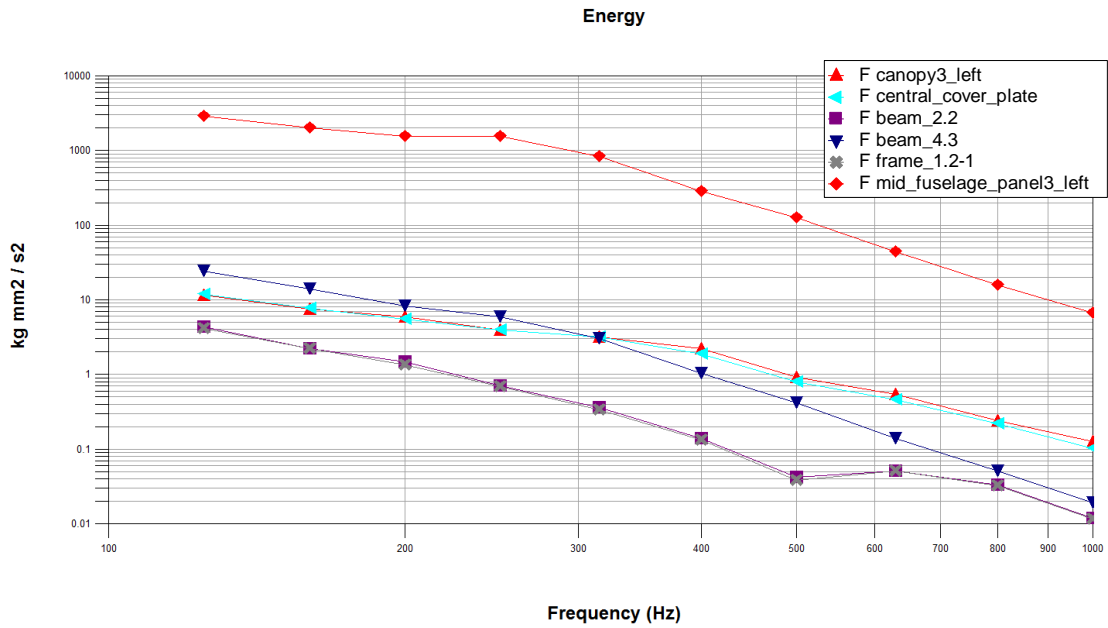


Figure 4.15 Energy level of SEA subsystems

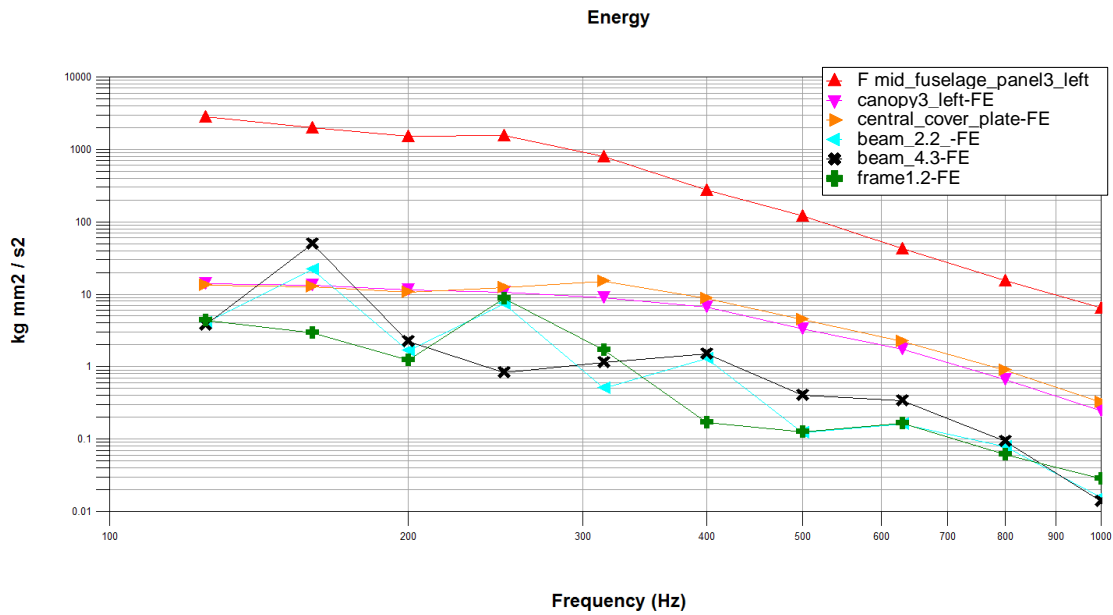


Figure 4.16 Energy level of FE-SEA hybrid parts

Another reason of this discrepancy could be that the hybrid FE-SEA method is used just to improve traditional SEA models for structure borne predictions. The reason for this act is that it allows to better capture the structural power input into stiff components and transmission through stiff and complicated parts. The simulation of the structural dynamic force through attachment points is represented better with FEM other than SEA method. For our analysis, the results obtained for both models by employing airborne power inputs. Therefore, it is not a case involving structure-borne transmission problems. Structure-borne noise is generally limited to the frequency range of 20 Hz-600 Hz. Airborne noise is generally limited above 400 Hz [3]. The efficiency of hybrid FE-SEA method is monitored better if any structure-borne power inputs exist. Hence, the results possibly differ more from the SEA results.

Additionally, the correlation between experimental target values and numerical one may not be achieved at low frequencies for both models in the validation step of SEA modelling. Because, especially up to 400 Hz, all parts of the model should be modelled by pure FEM to get accurate results at this low frequency range. All the peaks in the sound pressure level predictions can be established if FE method is used. Therefore, an experimental study should be carried to make comments with higher confidence level, especially at low frequencies.

CHAPTER 5

CONCLUSIONS AND FUTURE WORK

5.1. Discussion of Results

In the SEA results, distinct peaks are identified with gear mesh frequencies and their harmonics. Additionally, the engine noise peak is found to appear at high frequencies.

The SEA model validation is included by comparing the results with the measured interior noise data of two rotorcrafts found in technical literature. The results are found to be compatible with similar helicopter interior noise levels. This implies the developed model in this study can be used as a base model for preliminary analysis.

Considering the whole helicopter structure, the main rotor and main gear box are on the upper side of the passenger cabin, therefore the path that noise propagates through is very short. Particularly, this region is under the highest pressure level at mid frequency range as presented in Figure 5.1. Thence, it is logical to mount noise insulation material on upper deck. Sound insulation effect on the helicopter body is observed.

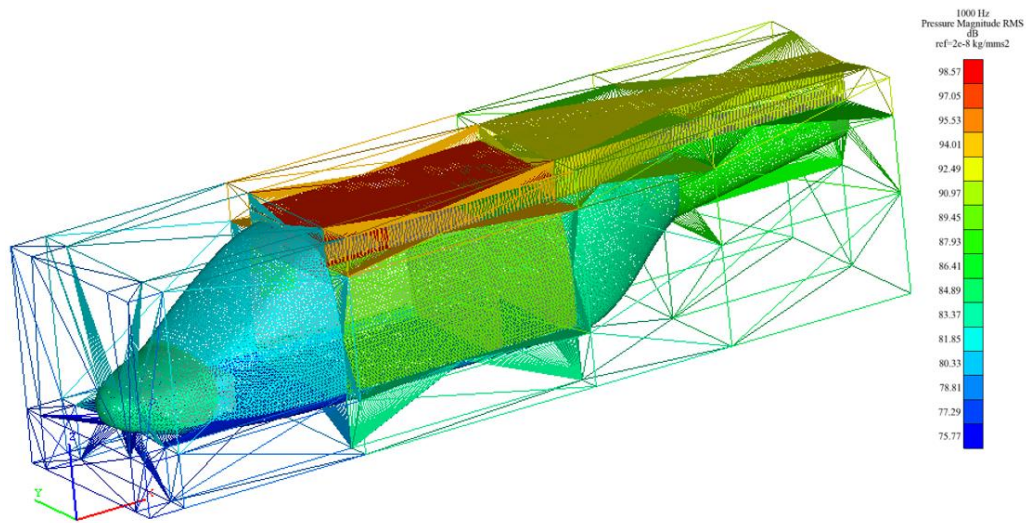


Figure 5.1 Sound energy flow in external cavities at 1000 Hz

Additionally, the hybrid model analysis is performed from 125 Hz to 1000 Hz. It is observed that noise levels at all frequencies are increased compared to those of SEA model. The reason of this result is that the sound energy storage capability is increased more by inclusion of higher number of resonant modes starting at 500 Hz band. In the overall result, the difference between the two models is nearly 2 dB. However, drawback of hybrid model is that it requires extensive calculation times, which are about 60 times longer than SEA model for cases covered in this thesis.

By combining FE and SEA, the detailed FEM model can be added to SEA model. It is usually used when a structural force is applied on a local point or to investigate the structure borne noise transmission. Though, there are only airborne noise inputs in the analysis of this thesis which may be a reason of minor difference between the SEA and hybrid prediction results.

5.2. Summary and Conclusions

In this study, primary helicopter noise sources and propagation mechanisms to the cabin space are reviewed. The various vibro-acoustic analysis techniques are summarized with their strengths and weaknesses. As a primary method SEA and also hybrid FEM-SEA method were introduced with their basic formulas and physics behind the theories. Application of different methods for various engineering construction from different industries are briefly reported. Following that cabin noise levels of TLUH helicopter were predicted implementing a statistical energy analysis method for full frequency range and a narrowband hybrid finite element analysis for the low 1/3rd octave bands. Two different SEA models are constructed to analyze cruise flight condition. The steps of modelling process of a helicopter for SEA and hybrid method are presented. In the hybrid modelling, partitioning is established by describing only the stiff parts as FE. The criteria for the selection methodology is explained.

It should be noted that the developed SEA model is consisted of essential subsystems which can be improved later by adding the more detail into the model. The cabin cavity can also be divided into more pieces to distinguish the pressure distribution inside the passenger cabin in the near future. The excitations and some parameters such as damping loss factor cannot be available in the period of design. Therefore, some of the power inputs is estimated based on research work available in the literature. The damping loss factors are assumed to be 0.02 for all structural subsystems and 0.01 for all cavities if any treatments do not exist.

It is needed to demonstrate that helicopter is compliant with the MIL-STD-1474 D limits for the cabin noise perceived by the crew. Table 5.1 presents the sound pressure level limits in octave bands according to MIL-STD-1474D that shall not exceed with negligible background noise compared to helicopter noise sources for a design gross weight less than 9070 kg [46]. The results of our SEA model is evaluated for maximum horizontal velocity at maximum continuous power. The interior noise levels are required to ensure that noise limits specified by MIL-STD-1474. Figure 5.2 is reported the values in octave bands

obtained from the SEA analysis for acoustically treated and untreated cases and comparison with the limit given by the MIL 1474 D. Compliance with the MIL rule is guaranteed when application of NCT exists with the green curve which is SEA results with NCT is below the black curve which represents the MIL standards. Additionally, flight members shall not be exposed to octave band levels exceeding 145 dB peak instant noise in the range 1 Hz to through 40 kHz. When examining the results, this requirement is also complied. As the last resort cabin acoustic levels can be reduced by using, if need arises, an ear protection system like suitable helmet. This is characterized by an insertion loss that attenuates the noise present inside the cabin to an acceptable value.

Table 5.1 MIL-STD-1474D Sound Pressure Limits

Octave Band (Hz)	Limits (dB)
63	116
125	106
250	99
500	91
1000	87
2000	82
4000	80
8000	85
16000	89

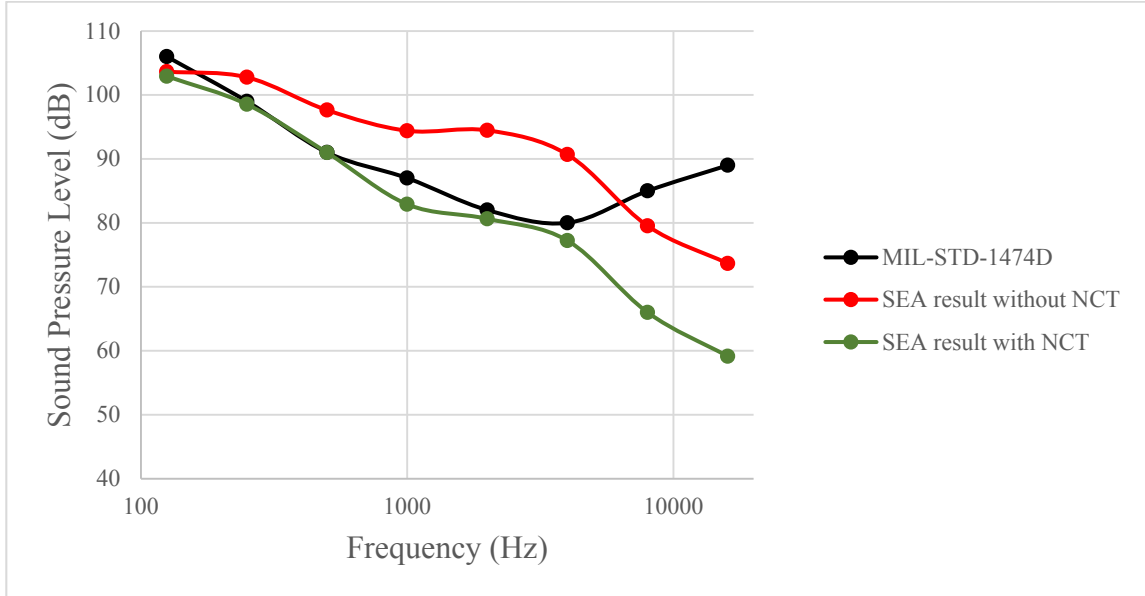


Figure 5.2 Comparison of SEA cabin noise prediction results with MIL standard

5.3. Recommendations for Future Work

As a future work, the model should be updated after the experimental evaluation. The model validation is vital to make a correct optimization. Furthermore, identification of transmission path to the passenger cabin should be done to find the most contributing path. Another improvement to the existing model is to define the power inputs after measuring acceleration or pressure levels of operational flight conditions at source location. The absorption coefficients of structural elements could also be determined with impedance tubes and this values could be projected to the properties of SEA subsystems.

For rotorcrafts, there are various type of structure with different materials. One of the main assumptions in our SEA model is the definition of constant damping values for all frequency range in 1/3 octave band and also for all subsystems if there does not exist any treatment. Therefore, an improvement to the existing approach is to measure the damping characteristic of the vehicle parts by experiments. Improved fundamental understanding of absorption materials is important to obtain better estimates of interior noise levels. The

half-power bandwidth method is currently the most widely used method for damping identification. With more realistic damping loss factors the response of the subsystems becomes more accurate since it is directly related to damping coefficient. Moreover, the damping of interior acoustic space which manifests itself as acoustic absorption can also be calculated.

Whilst the modelling, there are many simplifications done in order to build SEA model as simple as possible. It is essential to validate the SEA model by experiment. In validation process, the simulation results can be compared against operational measurements. However, it is firstly needed to characterize the input power from sources to include SEA model. Therefore, it can take long time and pose a few difficulties. Apart from this, a simple test configuration with a broadband noise source outside the vehicle or with an impact hammer can be set before the first flight. The baseline validation of the model may consist of taking the acoustic-acoustic or structural-acoustic transfer functions and confirming these with SEA model results exciting by the same inputs. Calculations of transfer functions or frequency response functions are carried between an input signal and the sound pressure level at the cabin cavity. This serves as a reference for the validation of the SEA simulation results. All these works are invaluable when the optimization process starts.

REFERENCES

- [1] Zaporozhets O., Tokarev V., Attenborough K., *Aircraft Noise Assessment, Prediction and Control*. Spon Press, (2011).
- [2] Rekos N.F., Large J.B., Lawson M.V., Ribner H.S., *Aircraft Noise Generation, Emission and Reduction*. AGARD Lecture Series No.77, (1975).
- [3] Wang X., *Vehicle noise and vibration refinement*, Oxford: CRC Press, (2010).
- [4] Caillet J., Marrot F., Malburet F., Carmona J-C., *Diagnosis and modelling of interior noise in helicopter cabins*, 31st European Rotorcraft Forum, Florence, (2005).
- [5] Butts D. J., *SEA interior noise validation for rotorcraft*, Dynamics and Internal Acoustics, Sikorsky Aircraft Corporation, (2008).
- [6] Mucchi E., Vecchio A., *Acoustical signature of a helicopter cabin in steady-state and run up operational conditions*, Measurement, Volume 43, Issue 3, 283-293, (2010).
- [7] Schatz R., Heger R., Korntheuer P., *EC145 Mercedes-Benz style with advanced interior acoustics*, Airbus Helicopters Deutschland GmbH, (2012).
- [8] Grosveld F.W., Cabell R.H., Boyd D.D., *Interior noise predictions in the preliminary design of the large civil tiltrotor (LCTR2)*, 69th Annual American Helicopter Society Forum and Technology Display, (2013).

- [9] Simpson R.N., Scott M.A., Taus M., Thomas D.C., Lian H., *Acoustic isogeometric boundary element analysis*, Journal of computer methods in applied mechanics and engineering, Volume 269, 265-290, (2014).
- [10] Beskos D.E., *Boundary Element Methods in Dynamic Analysis*, Journal of Applied Mechanics Reviews, Volume 40, 2-23, (2009).
- [11] Davidsson P., *Structure-Acoustic Analysis; Finite element modelling and reduction methods*, Doctoral Thesis, Lund University, (2004).
- [12] Lyon R., Dejong R., *Theory and Applications of Statistical Energy Analysis*, Butterworth-Heinemann, Second Edition, (1995).
- [13] Lyon R., Maidanik G., *Power flow between linearly coupled oscillators*, Journal of Acoustical Society of America, Volume 34, 640-647, (1962).
- [14] Woodhouse J., *An introduction to statistical energy analysis of structural vibration*, Journal of Applied Acoustics, Volume 14, 455-469, (1981).
- [15] Fahy F.J., *Statistical energy analysis: a critical overview*, Phil. Trans. R. Soc. Lond. A 346, 431-447, (1994).
- [16] Renji K., *On the number of modes required for statistical energy analysis-based calculations*, Journal of Sound and Vibration 269, 1128-1132, (2004).
- [17] Langley R.S., *A derivation of the coupling loss factors used in statistical energy analysis*, Journal of Sound and Vibration, Volume 141, 207-219, (1990).
- [18] Mace B.R., Rosenberg J., *The SEA of two coupled plates: an investigation into the effects of subsystem irregularity*, Journal of Sound and Vibration, Volume 212, 395-415, (1998).
- [19] Maidanik G., *Response of ribbed panels to reverberant acoustic fields*, Journal of the Acoustical Society of America 34, 809, (1962).

- [20] Shorter P.J., Langley R.S., *Vibro-acoustic analysis of complex systems*, Journal of Sound and Vibration, Volume 288, 669-699, (2005).
- [21] Langley R.S., Cordioli J.A., *Hybrid deterministic-statistical analysis of vibro-acoustic systems with domain couplings on statistical components*, Journal of Sound and Vibration, Volume 321, 893-912, (2009).
- [22] Cotoni V., Shorter P., Langley R., *Numerical and experimental validation of a hybrid finite element-statistical energy analysis method*, Journal of the Acoustical Society of America, Volume 122, 259-70, (2007).
- [23] Langley R.S., *A hybrid method for the vibration analysis of complex structural-acoustic systems*, Journal of the Acoustical Society of America, Volume 105, 1657, (1999).
- [24] Soize C., *A model and numerical method in the medium frequency range for vibroacoustic predictions using the theory of structural fuzzy*, Journal of the Acoustical Society of America, Volume 64, 849, (1993).
- [25] Belyaev A.K., Palmoc V.A., *Integral theories of random vibration of complex structures*, Journal of Studies in Applied Mechanics, Volume 14, 19-38, (1986).
- [26] Roibas-Millan E., Chimeno-Manguan M., Martinez-Calvo B., Lopez-Diez J., Fajardo P., Fernandez M.J., Simon F., *Criteria for mathematical model selection for satellite vibro-acoustic analysis depending on frequency range*, Conference paper of European Space Agency, (2012).
- [27] Peiffer A., Moeser C., Röder A., *Transmission loss modelling of double wall structures using hybrid simulation*, AIA-DAGA, Merano, (2013).
- [28] Perazzolo A., Costa A., *Interior acoustic design of the helicopter*, Acoustic and Vibration dept., AgustaWestland, Italy, (2006).

- [29] Kiremitçi U., *Interior and Exterior Noise Analysis of a Single Engine Propeller Aircraft Using Statistical Energy Analysis Method*, Master Thesis, Middle East Technical University, (2009).
- [30] Perazzolo A., Cenedese F., *Simulation and evaluation of noise and vibration reduction techniques in a helicopter cabin using SEA*, Acoustic and Vibration Department, AgustaWestland, Italy, (2005).
- [31] Cordioli J.A., Gerges S., Pererira A.K., *Vibro-acoustic modeling of aircrafts using statistical energy analysis*, SAE Technical Papers, (2004).
- [32] Bonilha M.W., Han F., *Application of predictive and experimental SEA to a S-92 helicopter sidewall section*, American Institute of Aeronautics and Astronautics, USA, (2000).
- [33] Lalor N., *Practical considerations for the measurements of internal and coupling loss factors on complex structures*, ISVR Technical Report No. 182, June, (1990).
- [34] Heron K.H., *Predictive SEA using line wave impedances*, IUTAM Symposium on Statistical Energy Analysis, volume 67, 107-118, (1999).
- [35] Cordioli J.A., *Modelling process and validation of Hybrid FE-SEA method to structure-borne noise paths in a trimmed automotive vehicle*, SAE Brasil Noise and Vibration Conference, (2008).
- [36] Gardner B., Cordioli J.A., Carneal J.P., *Advanced modeling of aircraft interior noise using the hybrid FE-SEA method*, Conference Paper, (2008).
- [37] VA One 2016.5, User's Guide, ESI Software, (2016).
- [38] Bremner P.G., Burton T.E., Cunningham A., *AutoSea2- A new design evaluation tool for noise and vibration engineering*, ASME, (1999).

- [39] Juang T., Vibrational and acoustic response of ribbed plates, Retrospective Theses and Dissertations, Iowa State University Capstones, (1993).
- [40] Mixson J.S., Wilby J.F., Interior Noise, NASA Langley Research Center, (1991).
- [41] Cordioli J.A., *Modelling process and validation of Hybrid FE-SEA method to structure-borne noise paths in a trimmed automotive vehicle*, SAE Brasil Noise and Vibration Conference, (2008).
- [42] Roibas-Millan E., Chimeno-Manguan M., Martinez-Calvo B., Lopez-Diez J., Fajardo P., Fernandez M. J. , Simon F., *Criteria for mathematical model selection for satellite vibro-acoustic analysis depending on frequency range*, Universidad Politecnica de Madrid, Universitat Politecnica de Valencia, Spain, (2012).
- [43] Laskin I., Orcutt F.K., Shipley E.E., *Analysis of noise generated by uh-1 helicopter transmission*, U.S. Army Aviation Material Laboratories, June, (1968).
- [44] P.D., Averbuch A., Raspet R., *Operational noise data for uh-60a and ch-47c army helicopters*, U.S. Army Aviation Material Laboratories, June, (1982).
- [45] Pollard J.S. Leverton J.W., *Cabin noise reduction- use of isolated inner cabins*, Westland Helicopters, England, (1976).
- [46] Department of Defense, "Noise Limits", Design Criteria Standard, MIL-STD-1474D, (1997).